

12-2017

# MPPT Control for Solar Splash Photovoltaic Array

Kelsey Zenko

Follow this and additional works at: <http://scholarworks.uark.edu/meeguht>



Part of the [Power and Energy Commons](#)

---

## Recommended Citation

Zenko, Kelsey, "MPPT Control for Solar Splash Photovoltaic Array" (2017). *Mechanical Engineering Undergraduate Honors Theses*. 67.  
<http://scholarworks.uark.edu/meeguht/67>

This Thesis is brought to you for free and open access by the Mechanical Engineering at ScholarWorks@UARK. It has been accepted for inclusion in Mechanical Engineering Undergraduate Honors Theses by an authorized administrator of ScholarWorks@UARK. For more information, please contact [scholar@uark.edu](mailto:scholar@uark.edu), [ccmiddle@uark.edu](mailto:ccmiddle@uark.edu).

# MPPT Control for Solar Splash Photovoltaic Array

An Honor thesis submitted in partial  
fulfillment of the requirements for the  
Honor Studies in Mechanical  
Engineering

by

Kelsey Zenko  
University of Arkansas  
Bachelor of Science in Mechanical Engineering,  
December, 2017

## **Abstract**

This thesis demonstrates the ability to model and simulate the operation of Maximum Power Point Tracking, MPPT. Moreover, the MPPT technology is contextualized within the confines of the Solar Splash competition to provide the foundation for future model development and simulation for optimal competition performance. MatLab Simulink was used to model the solar panel's operation. A MPPT algorithm was written using the perturb and observe method and was implemented in the model using a buck DC to DC converter. The performance of the model with hardware in the loop using Typhoon and dSPACE, which demonstrated how the actual hardware would operate in real time. The results showed that in Simulink, an idealized environment, the MPPT operates as expected. However, hardware simulation revealed inaccuracies of MPPT at lower irradiance values. For all cases, the driving force for changes in power is the value of irradiance.

**Acknowledgements**

Thank you to the University of Arkansas for the occasion to participate in the Honors Research program. I would like to express my sincere gratitude to Dr. Yue Zhao for the opportunity to work on this project. Moreover, I would like to thank Muhammed Hammad Uddin for his constant guidance.

## Table of Contents

1	Introduction .....	1
1.1	Motivation .....	1
1.2	Objective .....	1
2	Background.....	2
2.1	Solar Energy .....	2
2.2	Photovoltaics .....	2
2.3	Solar Applications .....	2
2.4	Maximum Power Point Tracking .....	3
2.5	MPPT Methods .....	4
2.5.1	Perturb and Observe.....	4
2.6	DC to DC converter.....	5
2.6.1	Buck Converter .....	5
3	Model and Simulation .....	8
3.1	PV and IV curves of the solar array .....	8
3.1.1	Solar Configuration.....	8
3.1.2	PV and IV Curves .....	8
3.2	Model in Simulink.....	11
3.2.1	Methodology .....	11
3.2.2	Model Solar Array .....	11
3.2.3	MPPT Algorithm .....	11
3.2.4	DC to DC Buck Converter Design.....	13
3.2.5	Model Overview .....	15

4	Model Results .....	16
4.1	Results at MPP Conditions.....	16
4.2	Results with Multiple Irradiance at 25°C .....	19
4.3	Results with Multiple Irradiance at 1000 W/m <sup>2</sup> .....	22
5	Hardware Simulation .....	24
5.1	Typhoon HIL and dSPACE .....	24
5.2	Solar Panels in Hardware .....	24
6	Hardware Results .....	27
6.1.1	Power: Changing Temperature .....	28
6.1.2	Power: Changing Irradiance .....	31
6.1.3	Voltage and Current: Changing Temperature .....	34
6.1.4	Voltage and Current: Changing Irradiance .....	35
7	Conclusion .....	36
	References .....	37
	Appendix 1: Grape Solar 100 W Specifications .....	39
	Appendix 2: MatLab Code for PO Method .....	41
	Appendix 3: Jinko Solar 200 W Specifications .....	42

## List of Figure

Figure 1 General PV Curve for Solar Array .....	3
Figure 2 General IV Curve for Solar Array .....	3
Figure 3 Circuit Schematic of a Buck Converter .....	5
Figure 4 Equivalent Circuit of Buck Converter when switch is On .....	6
Figure 5 Equivalent Circuit of Buck Converter when switch is Off .....	6
Figure 6 PV Curve for Multiple Irradiances at Constant Temperature .....	9
Figure 7 IV Curve for Multiple Irradiances at Constant Temperature .....	9
Figure 8 PV Curve for Multiple Temperatures at Constant Irradiance.....	10
Figure 9 IV Curve for Multiple Temperatures at Constant Irradiance.....	10
Figure 10 Simulink Block of Solar Array .....	11
Figure 11 Perturb and Observe (PO) Logic .....	12
Figure 12 P&O MPPT Controller Block in Simulink .....	12
Figure 13 Pulse Generator in Simulink .....	13
Figure 14 DC to DC Buck Converter in Simulink .....	14
Figure 15 Complete Simulink Model with Panels, MPPT, and DC/DC Converter .....	15
Figure 16 Power vs Time MPP Conditions .....	16
Figure 17 Voltage vs Time MPP Conditions .....	17
Figure 18 Current vs Time MPP Conditions .....	17
Figure 19 PV Curve: 1000 W/m <sup>2</sup> and 25°C .....	18
Figure 20 IV Curve: 1000 W/m <sup>2</sup> and 25°C .....	18
Figure 21 PV Curve: 750 W/m <sup>2</sup> and 25°C .....	19
Figure 22 IV Curve: 750 W/m <sup>2</sup> and 25°C .....	19

Figure 23 PV Curve: 500 W/m <sup>2</sup> and 25°C .....	20
Figure 24 IV Curve: 500 W/m <sup>2</sup> and 25°C .....	20
Figure 25 IV Curve: 250 W/m <sup>2</sup> and 25°C .....	21
Figure 26 IV Curve: 250 W/m <sup>2</sup> and 25°C .....	21
Figure 27 PV Curve: 1000 W/m <sup>2</sup> and 30°C .....	22
Figure 28 IV Curve: 1000 W/m <sup>2</sup> and 30°C .....	22
Figure 29 PV Curve: 1000 W/m <sup>2</sup> and 35°C .....	23
Figure 30 PV Curve: 1000 W/m <sup>2</sup> and 35°C .....	23
Figure 31 Percent Change in Pmax versus the Cell Temperature.....	25
Figure 32 IV and PV Curves at Different Values of Irradiance .....	26
Figure 33 Power versus Time: Simulation Reaching Steady State at 25°C and 1000 W/m <sup>2</sup> ....	27
Figure 34 Power versus Time: Increasing Temperature from 25°C to 35°C at 1000 W/m <sup>2</sup> .....	28
Figure 35 Power versus Time: Increasing Temperature from 35°C to 45°C at 1000 W/m <sup>2</sup> .....	29
Figure 36 Power versus Time: Increasing Temperature from 45°C to 55°C at 1000 W/m <sup>2</sup> .....	30
Figure 37 Power versus Time: Decreasing Irradiance from 1000 to 800 W/m <sup>2</sup> at 25°C .....	31
Figure 38 Power versus Time: Decreasing Irradiance from 800 to 600 W/m <sup>2</sup> at 25°C .....	32
Figure 39 Power versus Time: Decreasing Irradiance from 600 to 400 W/m <sup>2</sup> at 25°C .....	33
Figure 40 Voltage and Current Input and Output versus Time of Increasing Temperature from 25 to 55°C 1000 W/m <sup>2</sup> .....	34
Figure 41 Voltage and Current Input and Output versus Time of Decreasing Irradiance from 1000 to 500 W/m <sup>2</sup> at 25°C .....	35



## List of Table

Table 1 Perturb and Observe Logic .....	4
Table 2 100W Grape Solar PV panel .....	8
Table 3 L and C Calculations .....	14
Table 4 Jinko Solar JKM200M 200 Watt Solar Panel .....	24
Table 5 Temperature of Solar Panel Corresponding to the relative Change in Power and Value for Power.....	25
Table 6 Power Produced by Irradiance for two Jinko Solar JKM200M 200 Watt Solar Panels ..	26

# **1 Introduction**

## **1.1 Motivation**

Solar Splash is a nationwide competition for collegians. Many teams design and build a boat with power source solely comprised of solar energy. The boat will compete in three different competitions; endurance, sprint, and solar slalom. The endurance race has the boat travel as far as possible on the lake in two hours. The sprint race focuses on speed by timing how fast the boat can cover a 70-meter distance. The solar slalom focuses on the ability to maneuver the boat in a figure eight pattern as quick as possible [1]. These events happen over a four-day period, and therefore efficient charging of the batteries for these competitions is paramount.

The general electrical set up is a solar panel, batteries, and motor according to certain limits as stated in the rules [1]. This purposely leaves the design of the boat up to the discretion of the teams involved. Therefore, the motivation for this thesis is to be a first stepping stone to model and analyze the operation of an electrical system for the Solar Splash Competition.

## **1.2 Objective**

The objective of this research is to model and simulate in MatLab Simulink the operation of solar panels within a maximum power point tracking system.

## **2 Background**

### **2.1 Solar Energy**

Solar Energy, the energy produced by sunlight, is becoming an increasingly common source of energy. The demand for solar energy through the year 2020 is growing exponentially. Between the years 2015 and 2016 alone the global demand for solar power grew by 25.6% [2]. This demand for solar energy not only calls for improved technology but also investments in younger generations to fulfil those industry needs. Solar Splash is an example which engages undergraduate students with solar technology under the guise of fun and competition.

### **2.2 Photovoltaics**

Photovoltaics is a system defined by the photovoltaic effect which is the phenomenon of certain material to produce a voltage and current when exposed to the sunlight [3]. A common application of photovoltaics is solar panels or solar arrays. Solar panels are comprised of smaller cells made of silicon. Panels can be further categorized based on production as monosilicon, polysilicon or thin-film [4]. The number of cells that comprise a panel and the method of production varies widely according to the application.

### **2.3 Solar Applications**

Two main applications for solar arrays is grid-tie and stand-alone. Grid-tie is when the energy produced is tied into a grid, which is distributed to many consumers. High voltages and currents are typical for a grid-tie because the energy must be transported over long distances.

A stand-alone solar energy system is one that is not tied to the grid, rather it is closed to itself. Generally, the power for a stand-alone is much smaller when compared to a grid-tie. A solar boat which uses solar energy to charge batteries to power a motor is an example of a stand-alone system [5].

## 2.4 Maximum Power Point Tracking

Maximum Power Point Tracking, MPPT, is an essential step within a photovoltaic system by influencing the panels to operate at their maximum power. As shown by the Power versus Voltage, PV, curve, *Figure 1*, for a given irradiance level and temperature there is one maximum power.

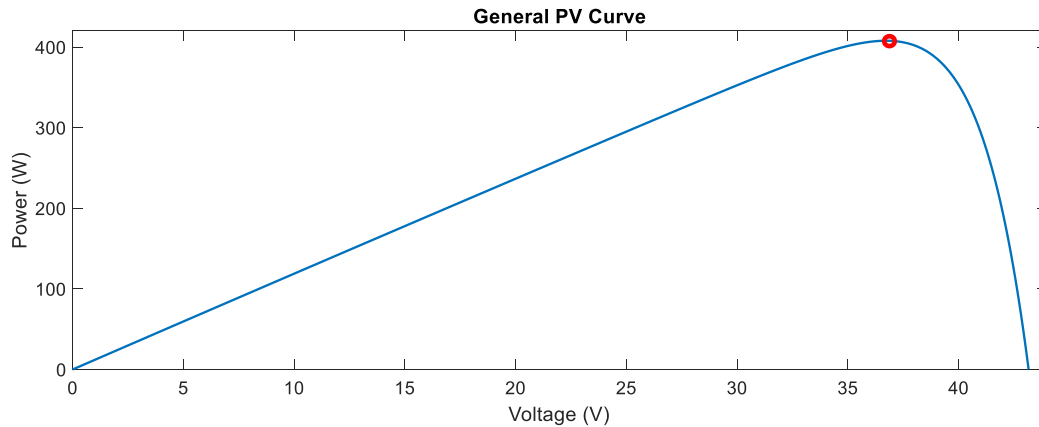


*Figure 1 General PV Curve for Solar Array*

That value for maximum power corresponds to a specific operating voltage and current shown by the IV curve in *Figure 2*.

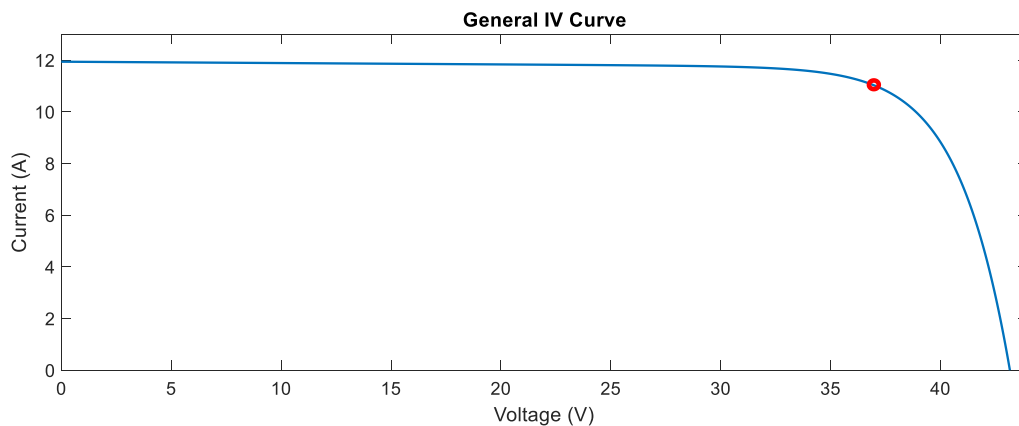


*Figure 2 General IV Curve for Solar Array*

The nature of photovoltaics is completely dependent upon the sun and weather conditions which are continually changing. Even on a cloudless day there is the inevitable rise and set of the

sun. Therefore, in reaction to different values for temperature and irradiance the power curve, while maintaining a similar shape, will scale itself accordingly. Moreover, the maximum power point is constantly changing. This illustrates the advantage of being able to track that maximum power point and control the operating point in a dynamic system [6].

## 2.5 MPPT Methods

There are many different methods of MPPT that have been developed. They have a similar goal to create a system that will automatically find the voltage and current at that specific irradiance and temperature that result in the maximum power [7]. Two of the most common MPPT methods are known as Perturb and Observe, PO, and Incremental Conductance, IC [8].

### 2.5.1 Perturb and Observe

Perturb and Observe method manipulates the duty ratio and reacts to how that perturbation affects the voltage and ultimately the power. A reduction in the duty ratio results in a lower voltage. Conversely, a rise in the duty ratio results in a higher voltage.

At the center of the PO method is that the system will be perturbed, and the resulting change in power is what determines the next perturbation. This method is also referred to as a ‘hill-climbing’ method. The shape of the PV curve, *figure 1*, is shaped like a single hill. To operate at the MPP the system is constantly taking a step and then checking if the power is higher or lower than its previous step. The logic of PO can be summarized in *table 1*, there are only four paths that the can be taken [9].

Previous Perturbation	Effect on Power	Next Perturbation
Increase	Increase	Increase
Increase	Decrease	Decrease
Decrease	Increase	Decrease
Decrease	Decrease	Increase

*Table 1 Perturb and Observe Logic*

This requirement to either decrease or increase with every step reveals an issue with PO in steady state. When the MPP is reached and the system is in steady state the value for power will not be constant, rather the power will oscillate around the MPP value [10].

## 2.6 DC to DC converter

A DC/DC converter is an electronic device that converts an input of direct current, DC, at one voltage to an output DC at another voltage. This has many different applications within power electronics. Comparable to a transformer that steps-up and steps-down AC power, the DC/DC converter can also be used to step-up voltage (boost), step-down voltage (buck), or both (buck-boost) [11].

### 2.6.1 Buck Converter

The Circuit diagram for a buck converter is shown in *figure 3*, where  $V_s$  is the input voltage.  $V_a$  is the average output voltage across the load resistance. A buck converter operates in two modes, when the switch is on and when the switch is off [12].

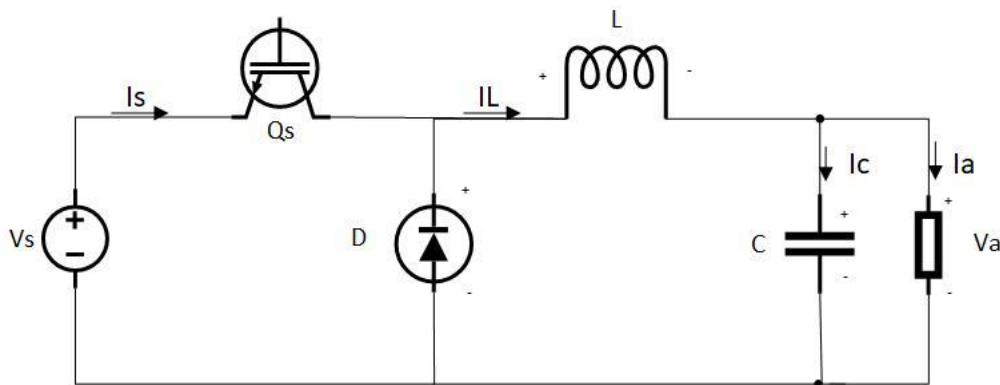


*Figure 3 Circuit Schematic of a Buck Converter*

Mode 1 is given by the equivalent circuit *figure 4* where  $Q_s$  is switched on.

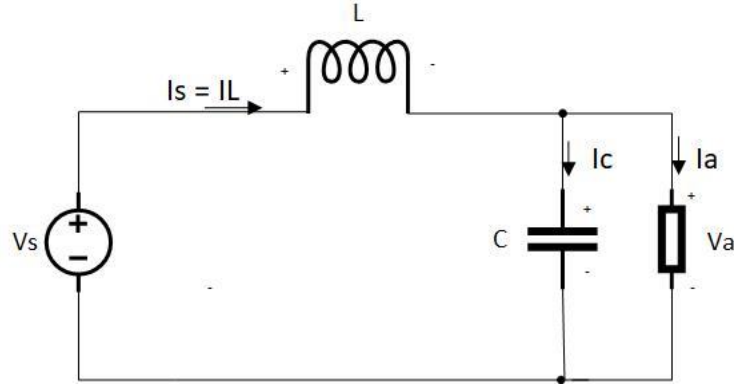


Figure 4 Equivalent Circuit of Buck Converter when switch is On

The amount of time in mode 1,  $t_{on}$ , is calculated through equation 1.

$$t_{on} = \frac{L \Delta I}{V_s - V_a} \dots \dots \dots (1)$$

Mode 2 is given by the equivalent circuit figure 5 where  $Q_s$  is switched on.

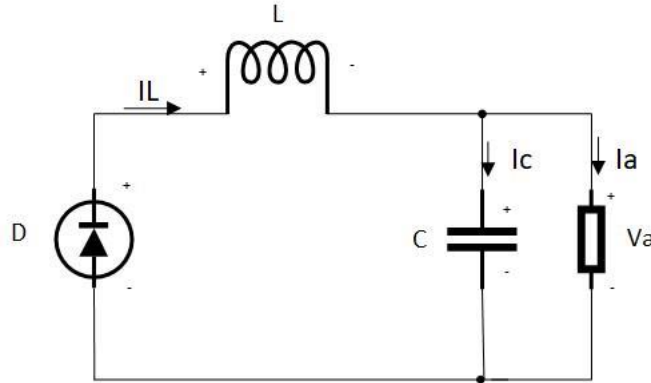


Figure 5 Equivalent Circuit of Buck Converter when switch is Off

The amountt of time in mode 2,  $t_{off}$ , is calculated through equation 2. Where delta I is the current ripple in the inductor.

$$t_{off} = \frac{L \Delta I}{V_a} \dots \dots \dots (2)$$

The switching period, T, or 1 over the switching frequency  $f_s$  is the sum of  $t_{on}$  and  $t_{off}$ .

$$T = \frac{1}{f_s} = t_{on} + t_{off} = \frac{LV_s \Delta I}{V_a(V_s - V_a)} \dots \dots \dots (3)$$

Where, the output voltage is a fraction of the input voltage. D is the duty cycle which is between 0 and 1, *equation 4*.

$$V_a = V_s D \dots \dots \dots (4)$$

Substitute *equation 4* into *equation 3* and rearrange to solve for L, the inductance value.

$$L = \frac{V_s D(1-D)}{f \Delta I} \dots \dots \dots (5)$$

The capacitor voltage,  $v_c$ , is given by *equation 6*.

$$v_c(t) = v_c(0) + \frac{1}{C} \int_0^{T/2} \frac{\Delta I}{4} \dots \dots \dots (6)$$

The integral from *equation 6* can be solved and the capacitor ripple voltage,  $\Delta v_c$ , determined, *equation 7*.

$$\Delta v_c = v_c(t) - v_c(0) = \frac{1}{C} \int_0^{T/2} \frac{\Delta I}{4} dt = \frac{\Delta I}{8 f_s C} \dots \dots \dots (7)$$

Substitute *equation 5* for the value of ripple current through the inductor,  $\Delta I$ , and rearrange to solve for C, the value of the capacitor, *equation 8*.

$$C = \frac{V_s D(1-D)}{8 L f_s^2 \Delta V} \dots \dots \dots (8)$$

*Equations 5 and 6* are necessary calculations for correctly sizing the capacitor and the inductor within the DC to DC buck converter.



### 3 Model and Simulation

#### 3.1 PV and IV curves of the solar array

##### 3.1.1 Solar Configuration

This model uses four 100 Watt solar panels where there are two parallel strings each with two panels in parallel. This produces a maximum power of 400 Watts. The manufacturer is Grape Solar, and this is the same solar configuration that was used in Solar Boat 2017 competition. The characteristics for one panel are given in *table 2* and the specification sheet for the solar panel is given in *Appendix 1*.

Maximum Power Pmax	100 W (-10%, +10%)
Voltage at Maximum Power Point Vmpp	17.8 V
Current at Maximum Power Point Impp	5.62 A
Open Circuit Voltage Voc	21.6 V
Short Circuit Current Isc	5.97 A
Temperature Coefficient of Voc	-0.28 %/°C
Temperature Coefficient of Isc	+0.04 %/°C

*Table 2 100W Grape Solar PV panel*

##### 3.1.2 PV and IV Curves

The PV and IV curves characteristic to the solar array described in section 4.2.1 of this thesis were modeled via the same method detailed in the “Comprehensive Approach to Modeling and Simulation of Photovoltaic Arrays” [13].

The MPP of the solar array occurs when the irradiance is at 1000 W/m<sup>2</sup> and the temperature is 25 °C. The graphs for how the power curve and corresponding current and voltage are affected by changes in the irradiance values are shown in *figures 6* and *7*.

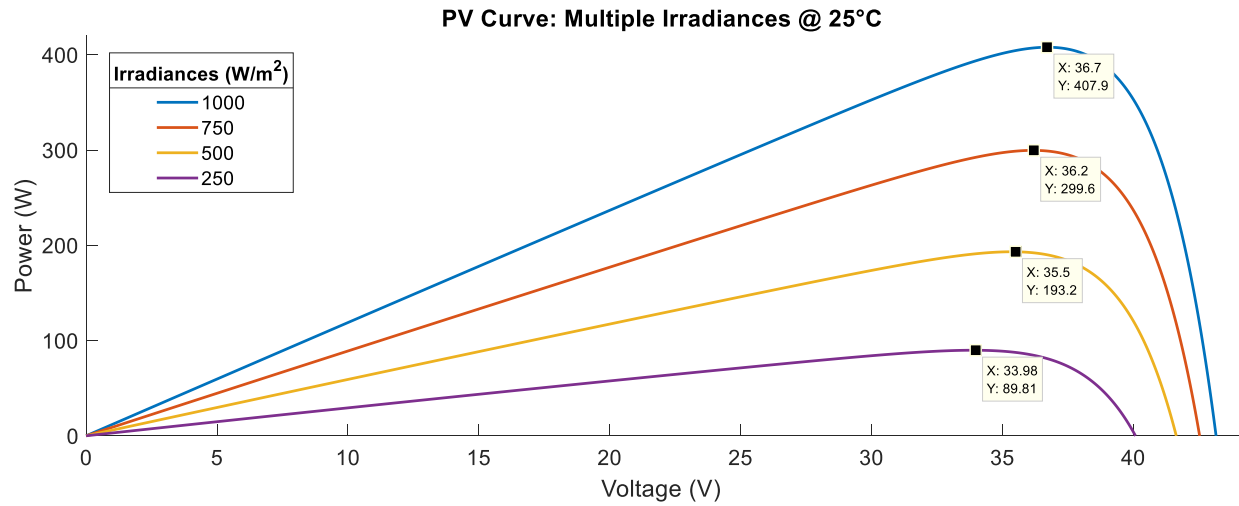


*Figure 6 PV Curve for Multiple Irradiances at Constant Temperature*

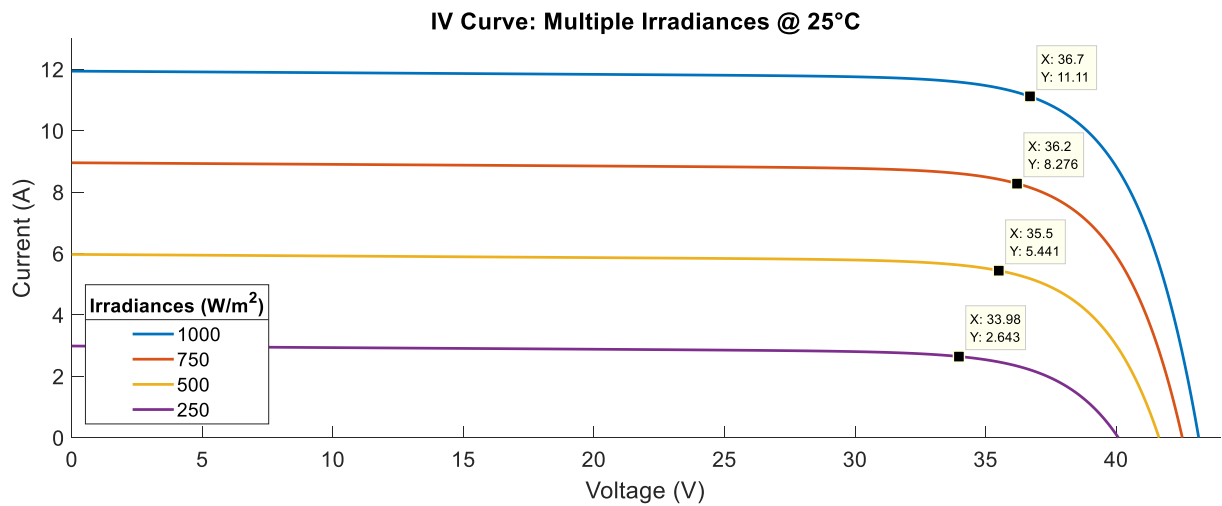


*Figure 7 IV Curve for Multiple Irradiances at Constant Temperature*

Figures 8 and 9 are the PV and IV curves for multiple temperatures and a constant irradiance value.

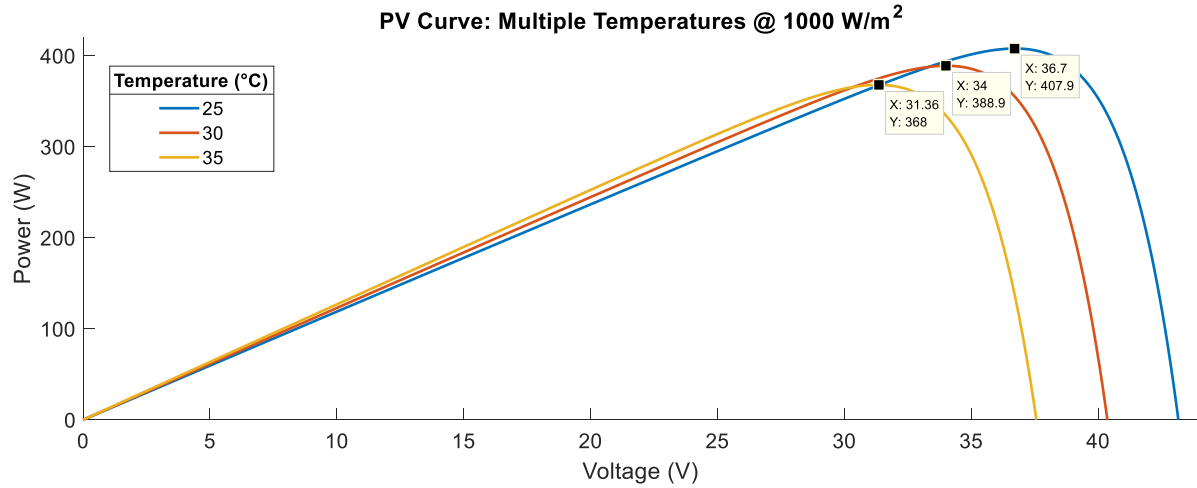


Figure 8 PV Curve for Multiple Temperatures at Constant Irradiance

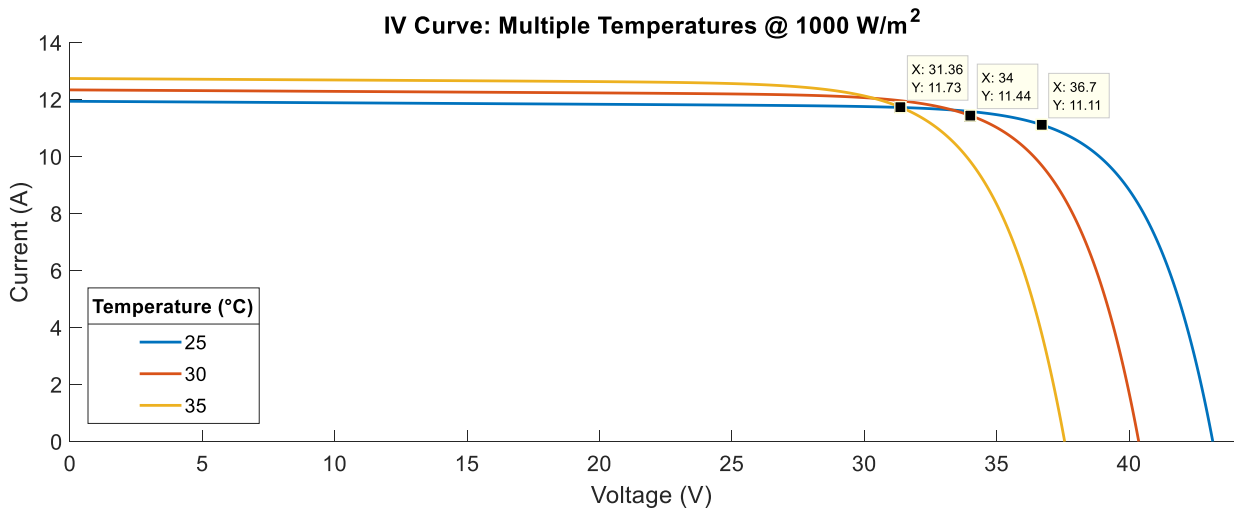


Figure 9 IV Curve for Multiple Temperatures at Constant Irradiance

## 3.2 Model in Simulink

### 3.2.1 Methodology

- Model solar array
- Implement MPPT algorithm
- Develop of the Buck DC/DC
- Produce IV and PV curves with MPPT and DC/DC

### 3.2.2 Model Solar Array

The same model for generating the characteristic PV and IV curves was also used to simulate the operation of the solar panels. *Figure 10* is the block as seen in Simulink with two input arrows temperature and irradiance. Temperature is measured in Kelvin, K, and irradiance is measured in Watts per meter squared,  $\text{W/m}^2$ . These are the input values that will be changed to evaluate the model at different conditions.

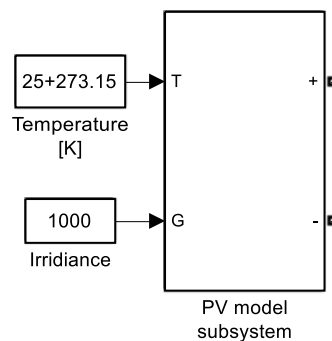


*Figure 10 Simulink Block of Solar Array*

### 3.2.3 MPPT Algorithm

Perturb and Observe was the chosen method of MPPT by providing a simple starting point for modeling. The logic of *Table 1* from section 3.5.1 of this thesis can be presented via the flow chart in *figure 11*. This step by step decision tree is the logic of the MatLab written code attached in Appendix 2.

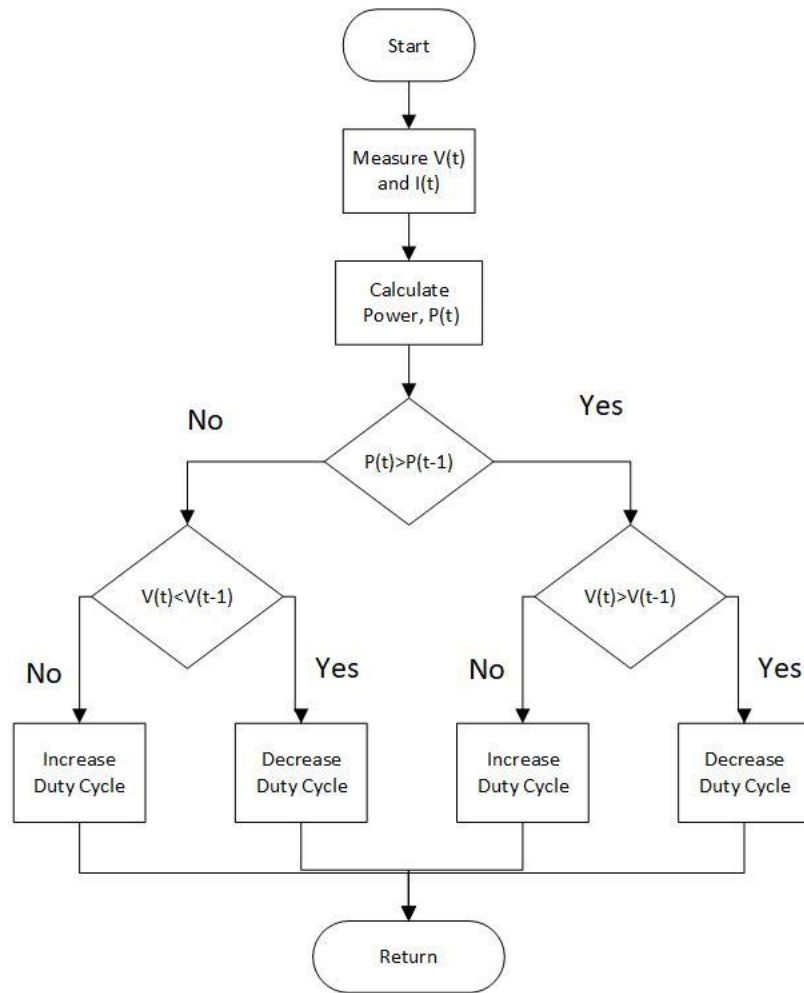


*Figure 11 Perturb and Observe (PO) Logic*

Within Simulink there is a block which creates a bridge between the MatLab workspace and the Simulink interface as shown in *figure 12*.

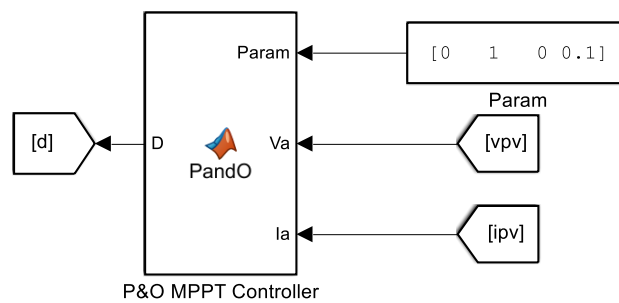


*Figure 12 P&O MPPT Controller Block in Simulink*

This block titled P&O MPPT Controller has three input arrows; Param, Va, and Ia. Param are four inputs for the PO code; Dinit, Dmax, Dmin, and deltaD. Dinit is the initial values for the duty cycle for the start of the simulation. Dmax and Dmin are the maximum and minimum values of the duty cycle, 1 and 0 respectively. Lastly, deltaD which is the amount each run of the code the duty cycle will be perturbed [14]. Va is the voltage measured across the solar panels and Ia is the current from the solar panels. The output arrow for the P&O MPPT Controller block is D, the value for duty cycle determined by the logic of the code.

This value for duty cycle, D, must be converted into a pulse for the input to the switch of the DC to DC converter. As shown in *figure 13* the value for duty cycle is input into the pulse generator also known as a pulse width modulator, PWM. The output is the pulse, g. The pulse is either on or off, the value for duty cycle changes the percentage the pulse is on in a period. Moreover, it controls the width. Within this block the switching frequency, f, of the system is established.

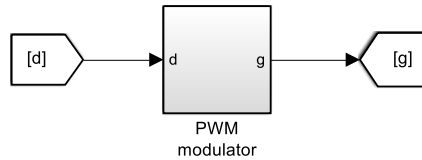


*Figure 13 Pulse Generator in Simulink*

### 3.2.4 DC to DC Buck Converter Design

Using *equations 5* and *8* the L and C values can be calculated for the model. The ripple current was approximated to be 5% of the total current at MPP. The ripple voltage was similarly approximated as 5% of the total voltage at MPP. The duty cycle, D, which ranges from a value of 0 to 1 was set to an average of 0.5. The switching frequency that was set within the model was 10000 Hz. Vs is the source voltage at MPP. *Table 3* summarizes these values and includes the resulting L and C values.

$\Delta I$	0.568 A
$V_s$	35.6V
D	0.5
f	10000 Hz
$\Delta V$	1.78 V
L	1.57 mH
C	3.9 $\mu$ F

*Table 3 L and C Calculations*

The DC to DC Buck Converter is what accomplishes the task of controlling the solar panels to the MPP determined by the MPPT algorithm. The model of the DC to DC Buck converter is shown in *Figure 14*, which mirrors the configuration of *figure 3* from section 3.7.1 of this thesis. The capacitor on the leftmost side of the circuit, C\_PV, is to smooth out the initial oscillation of the voltage exiting the solar panels. The value of capacitor C\_PV was set to a small value of 1  $\mu$ F.

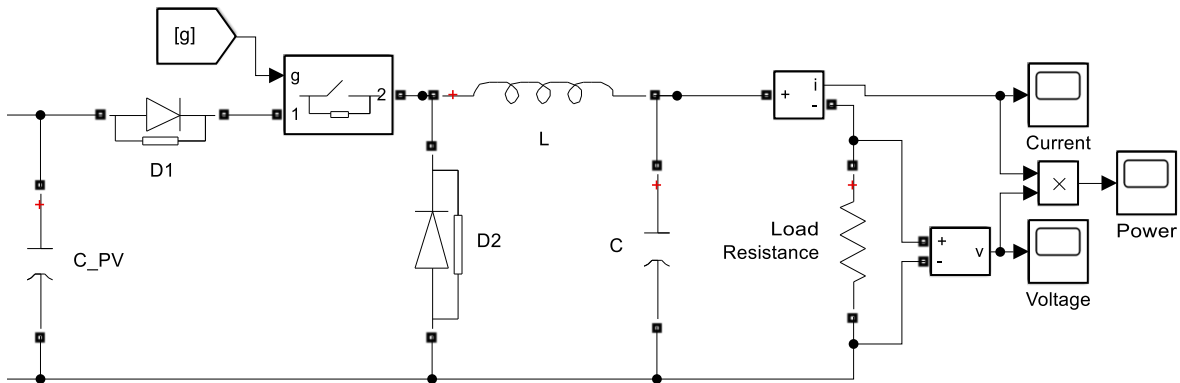


*Figure 14 DC to DC Buck Converter in Simulink*

*Figure 14* also shows on the right side the sampling of the resulting current and voltage, and the calculation for power using a multiplication operator in Simulink.

### 3.2.5 Model Overview

The model fully built in MatLab Simulink is shown in *figure 15*. The time step for the simulation is  $1\mu\text{s}$  shown in *figure 15* in the upper left-hand corner, the powergui block.

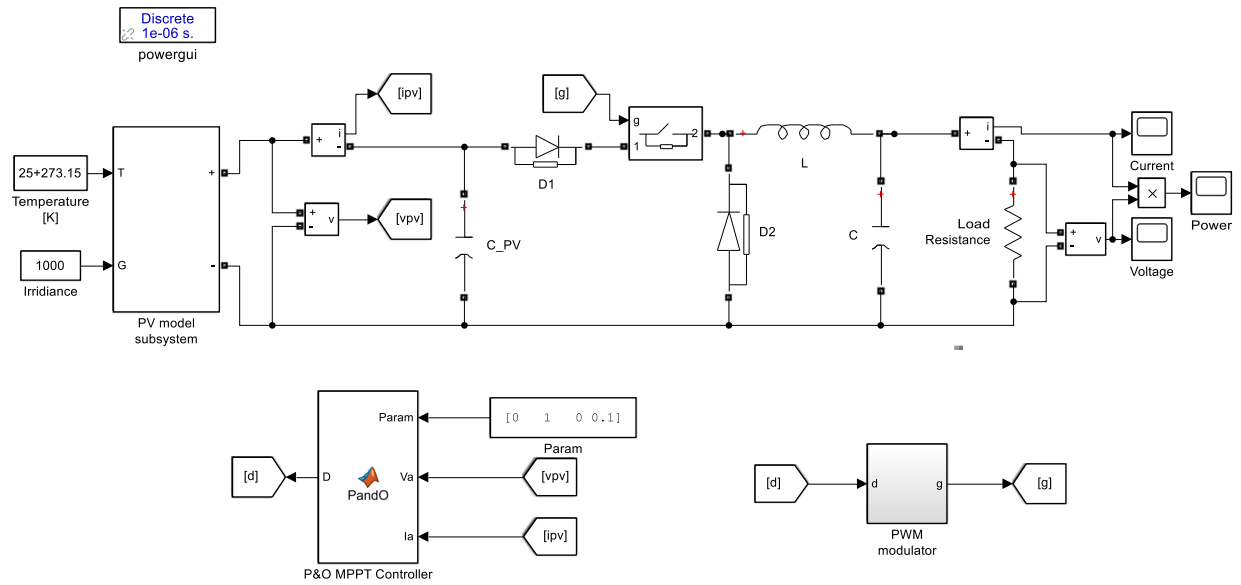


*Figure 15 Complete Simulink Model with Panels, MPPT, and DC/DC Converter*



## 4 Model Results

### 4.1 Results at MPP Conditions

At the MPP values of  $1000 \text{ W/m}^2$  and  $25^\circ\text{C}$  the model will be operating at peak performance. *Figures 16, 17, and 18* are the Power, Voltage and Current over a short span of 0.2 seconds. In all three graphs there is the initial increase in the values as the MPPT is climbing the hill working to find the maximum power. After the initial climb there is a constant oscillation which demonstrates the drawback of the PO method. This oscillation is minimized with proper sizing of the capacitor and the inductor.

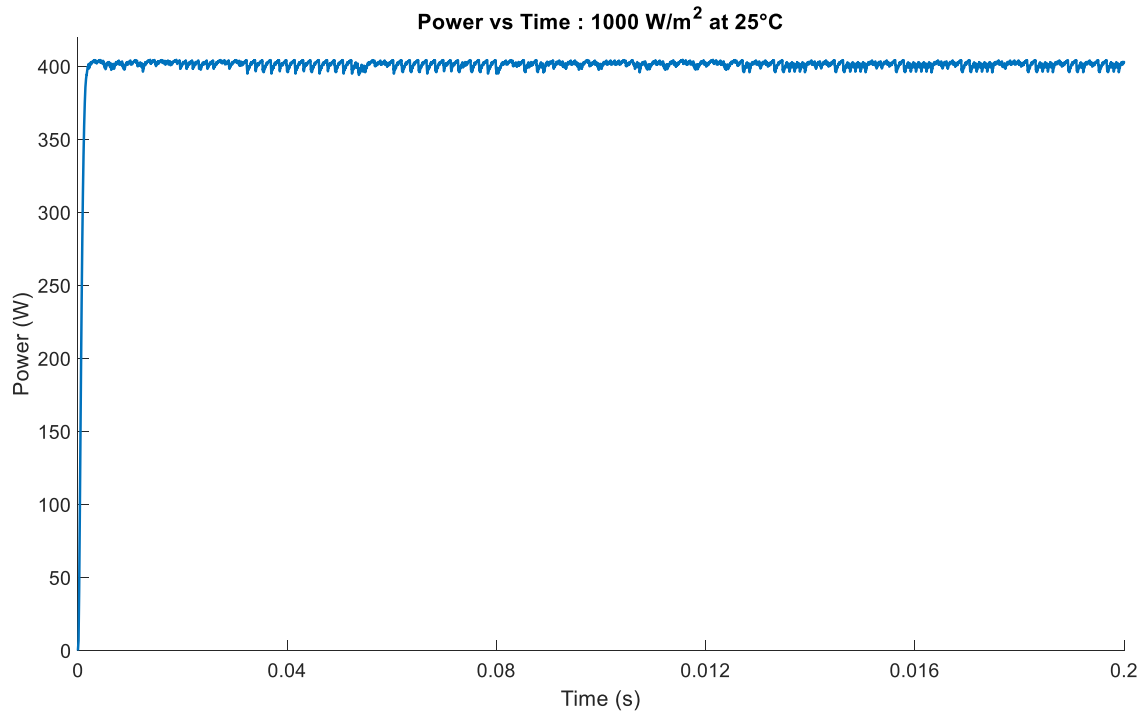


*Figure 16 Power vs Time MPP Conditions*

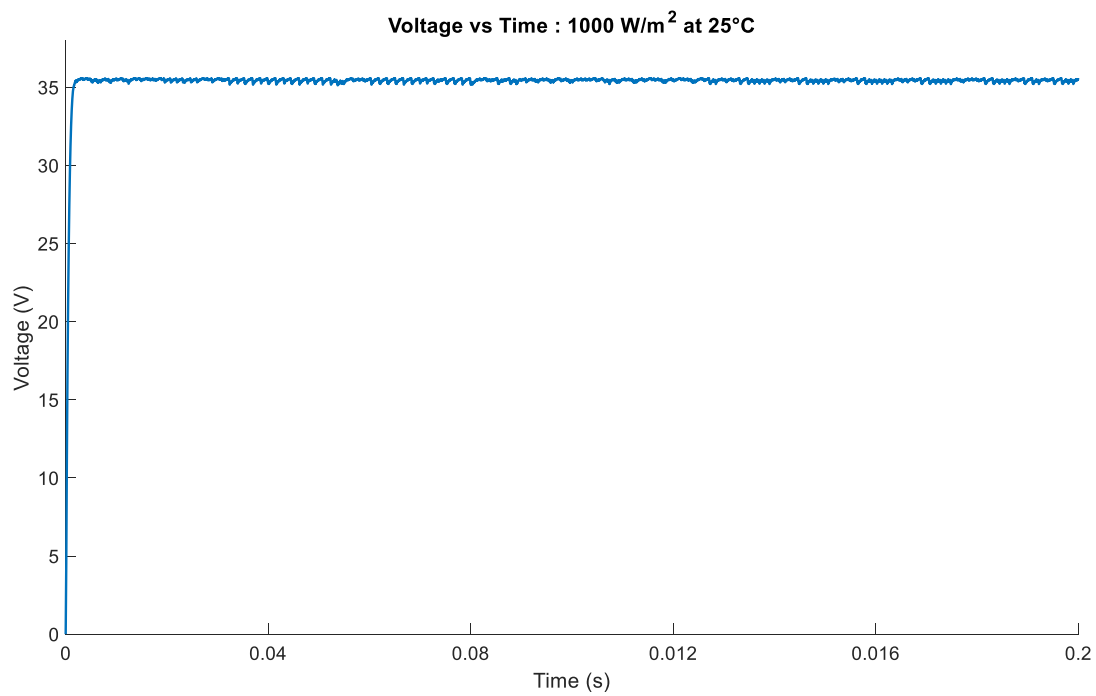


*Figure 17 Voltage vs Time MPP Conditions*

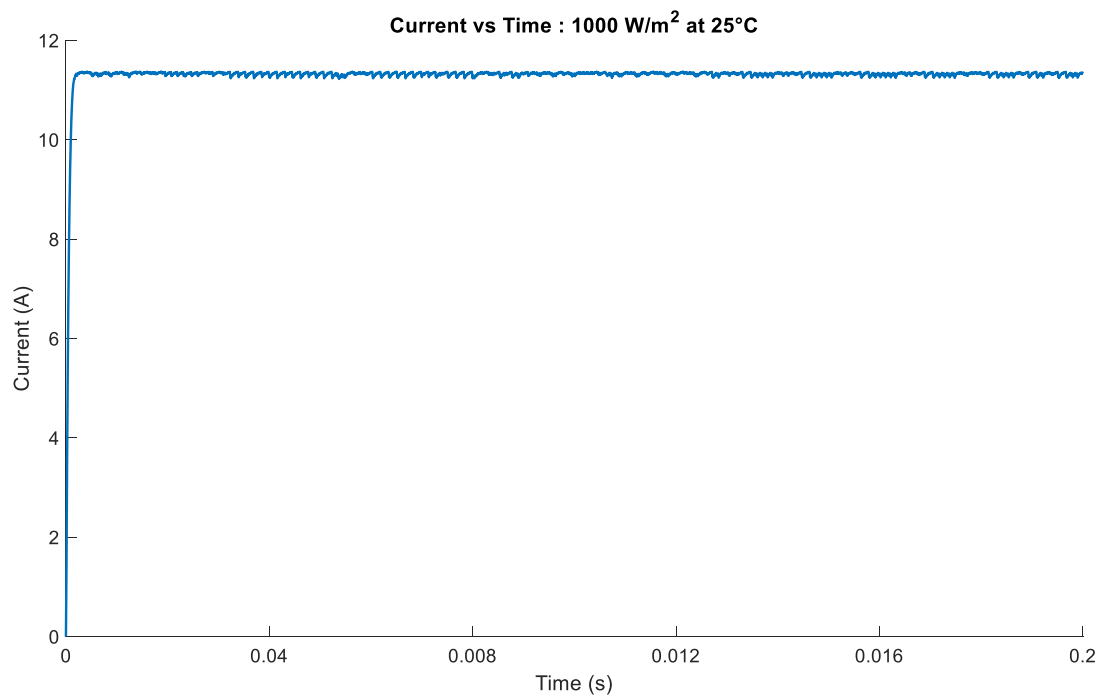


*Figure 18 Current vs Time MPP Conditions*

Figures 19 and 20 show the PV and IV curve generated by the panels themselves overlaid on the output values produced by the Simulink model. Each instance of the model output is represented by a circle. The circles at the beginning of the curve are spaced enough apart to see their shape. However, the oscillation around the MPP produces a cluster of points at the end of the curve. The important characteristic of the graph of the model output is not the shape, rather the distribution of points.

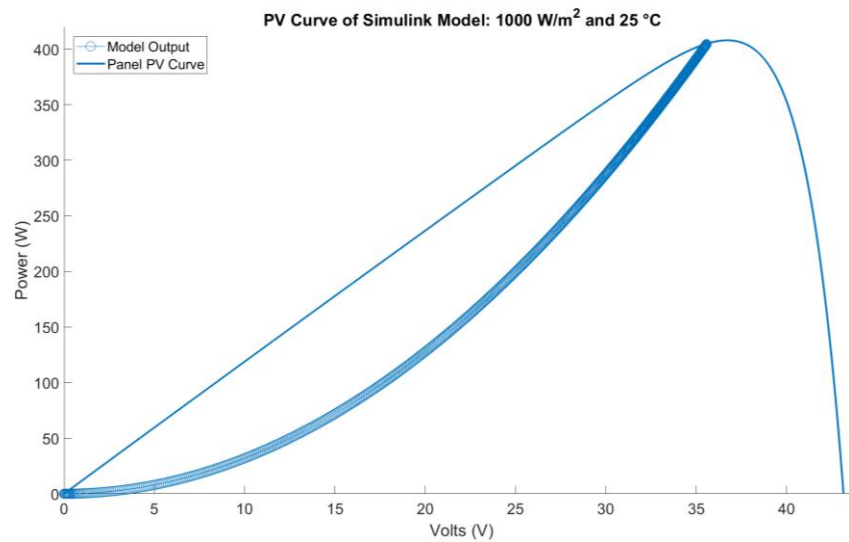


Figure 19 PV Curve: 1000 W/m<sup>2</sup> and 25°C

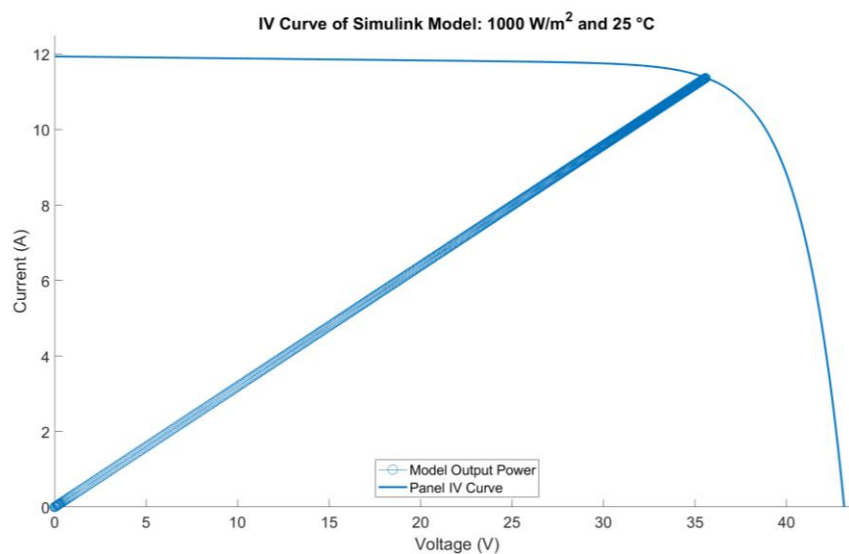


Figure 20 IV Curve: 1000 W/m<sup>2</sup> and 25°C

## 4.2 Results with Multiple Irradiance at 25°C

Figures 21 through 26 are plotted similarly to figures 19 and 20. Figures 21 and 22 are the PV and IV output when the value of irradiance is decreased to 750 W/m<sup>2</sup> and the temperature is constant at 25°C.

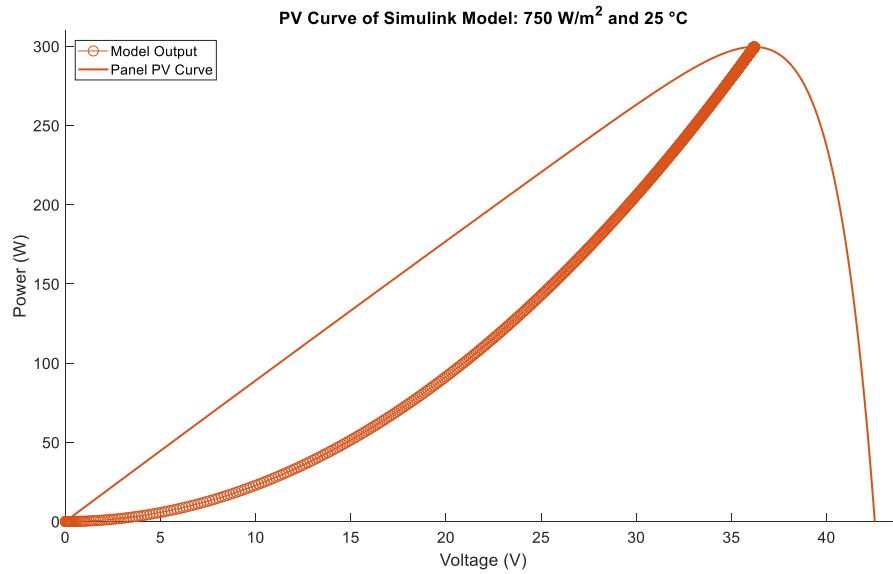


Figure 21 PV Curve: 750 W/m<sup>2</sup> and 25°C

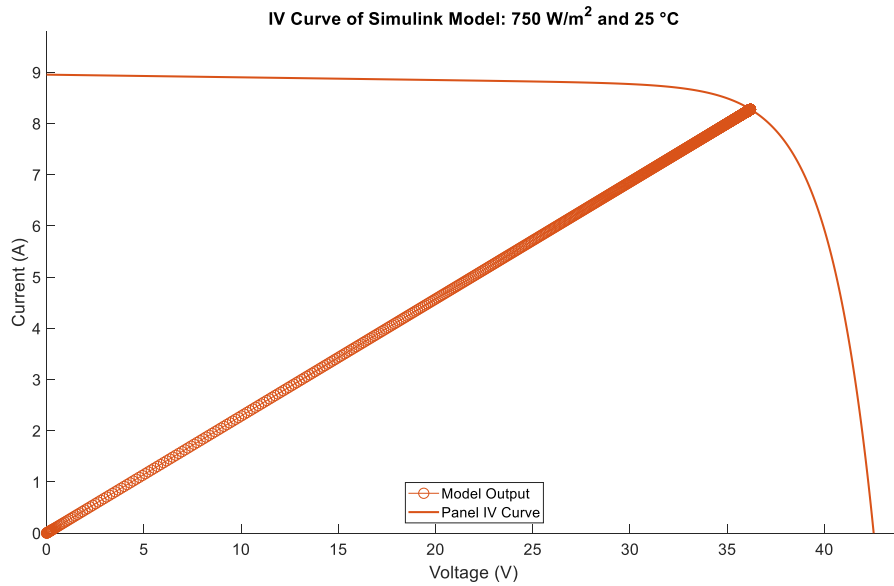


Figure 22 IV Curve: 750 W/m<sup>2</sup> and 25°C

Figures 23 and 24 are the PV and IV output when the value of irradiance is decreased to  $500 \text{ W/m}^2$  and the temperature is constant at  $25^\circ\text{C}$ .

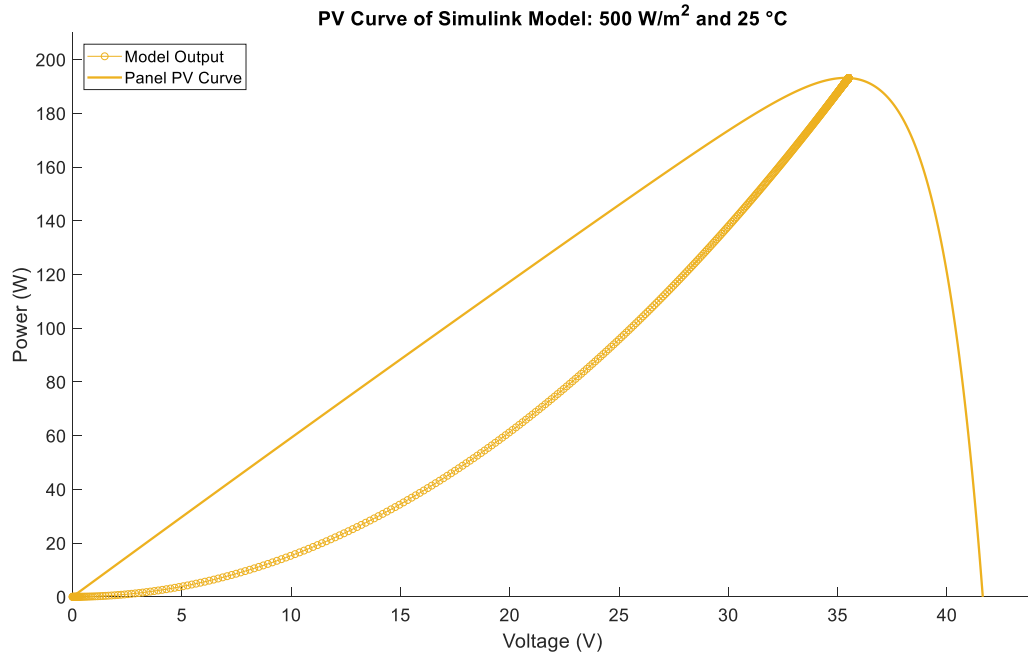


Figure 23 PV Curve:  $500 \text{ W/m}^2$  and  $25^\circ\text{C}$

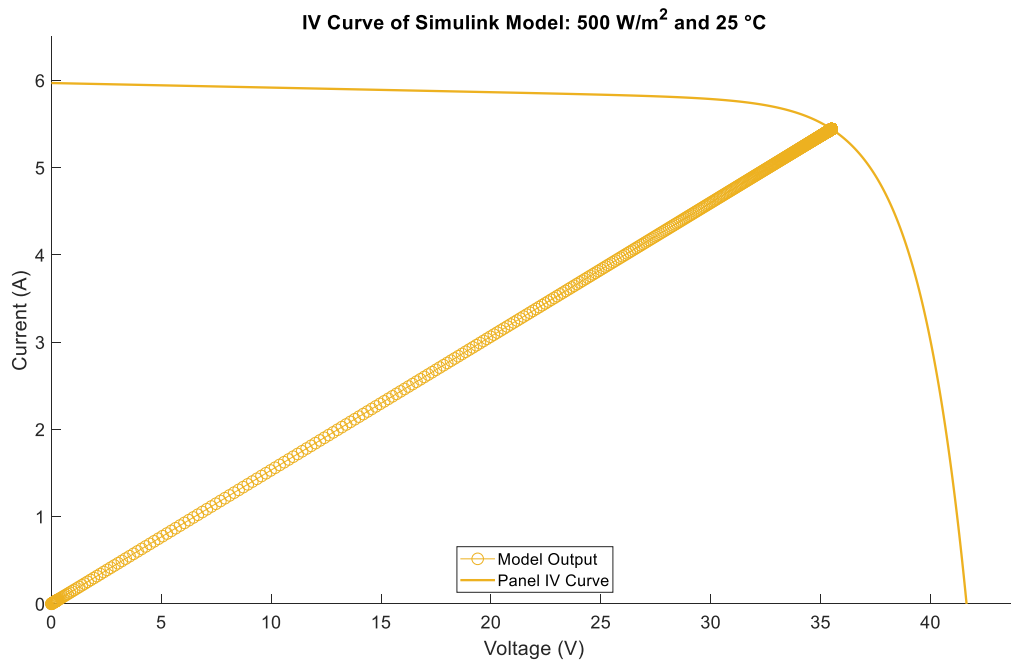
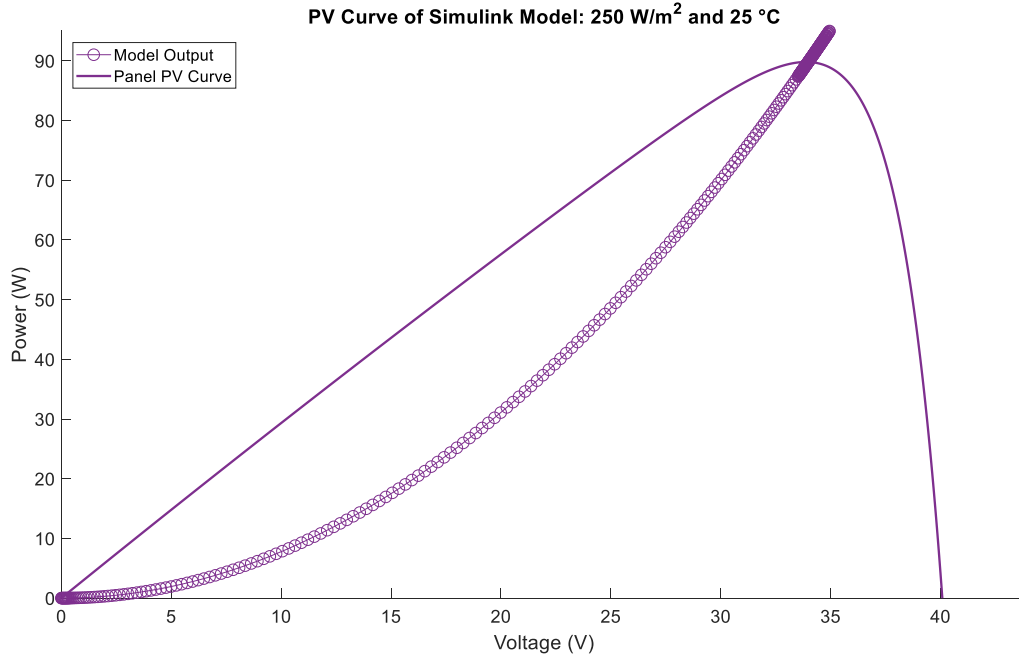
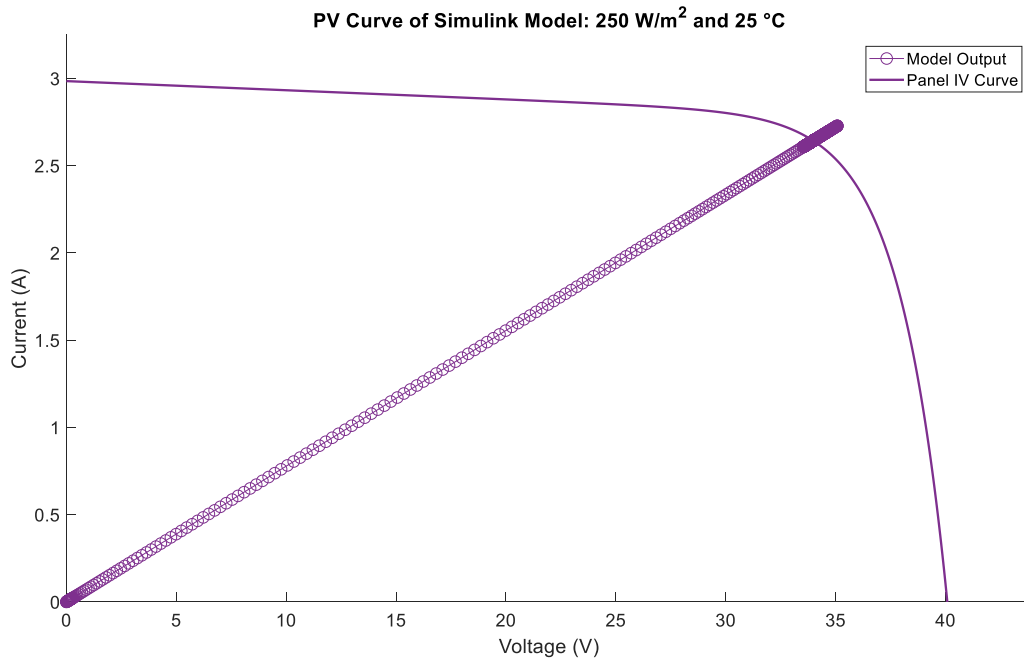


Figure 24 IV Curve:  $500 \text{ W/m}^2$  and  $25^\circ\text{C}$

Figures 25 and 26 are the PV and IV output when the value of irradiance is decreased to  $250 \text{ W/m}^2$  and the temperature is constant at  $25^\circ\text{C}$ .



*Figure 25 IV Curve:  $250 \text{ W/m}^2$  and  $25^\circ\text{C}$*



*Figure 26 IV Curve:  $250 \text{ W/m}^2$  and  $25^\circ\text{C}$*

### 4.3 Results with Multiple Irradiance at 1000 W/m<sup>2</sup>

Figures 27 through 30 are plotted similarly to figures 19 and 20. Figures 27 and 28 are the PV and IV output after the value of temperature is increased to 30°C and the irradiance is a constant 1000 W/m<sup>2</sup>.

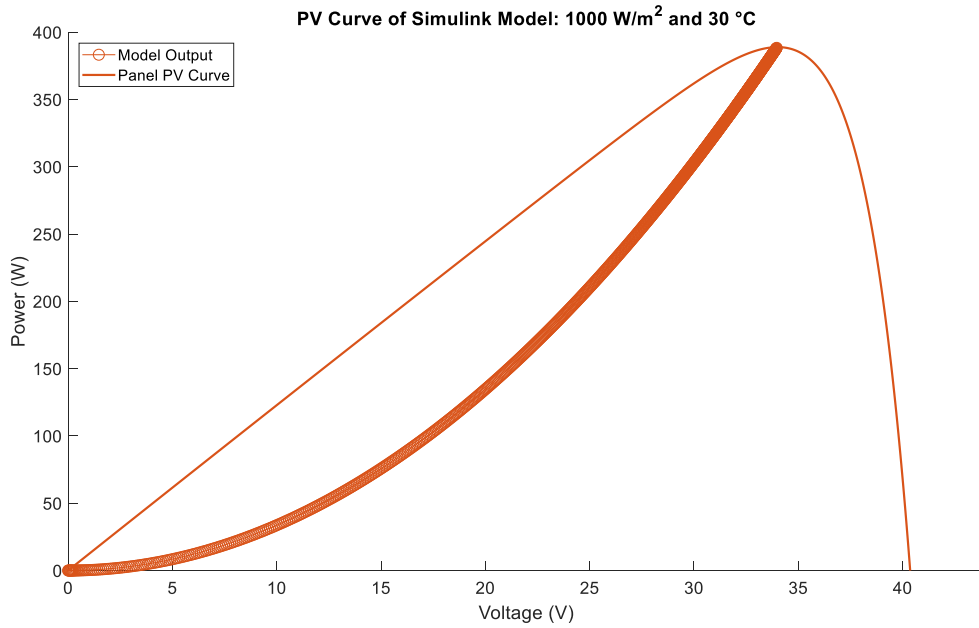


Figure 27 PV Curve: 1000 W/m<sup>2</sup> and 30°C

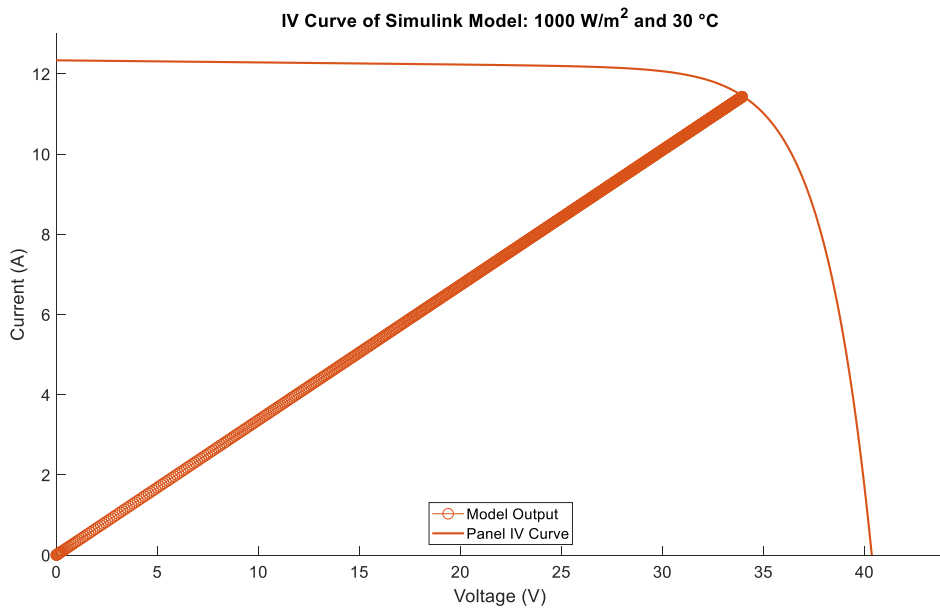


Figure 28 IV Curve: 1000 W/m<sup>2</sup> and 30°C

Figures 29 and 30 are the PV and IV output after the value of temperature is increased to 35°C and the irradiance is a constant 1000 W/m<sup>2</sup>.

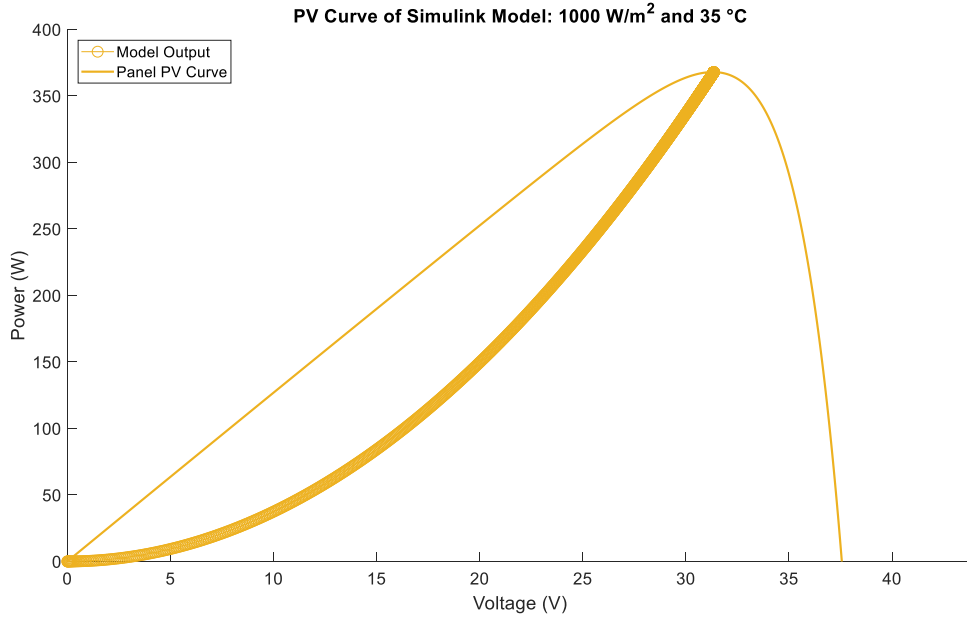


Figure 29 PV Curve: 1000 W/m<sup>2</sup> and 35°C

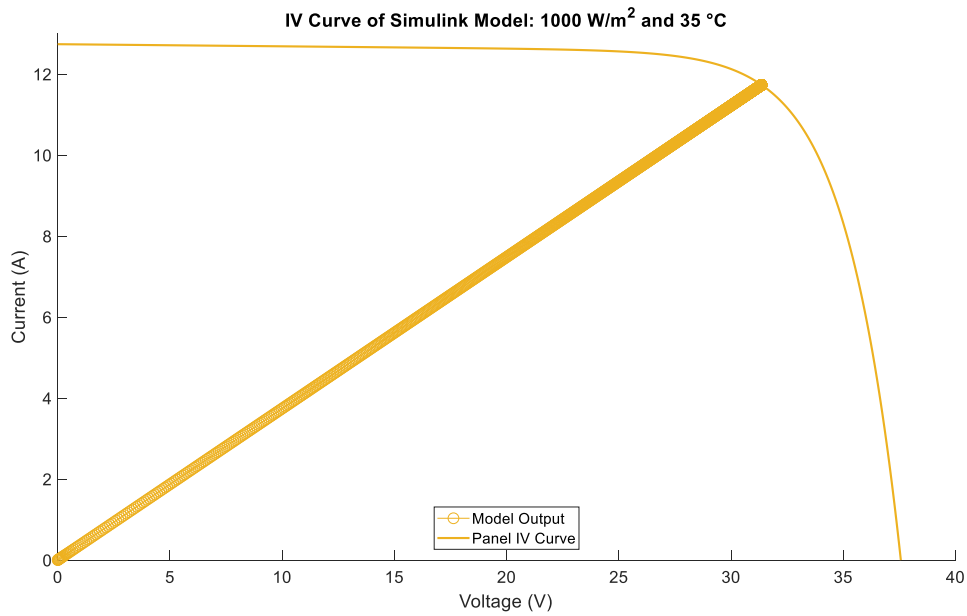


Figure 30 PV Curve: 1000 W/m<sup>2</sup> and 35°C



## 5 Hardware Simulation

### 5.1 Typhoon HIL and dSPACE

Typhoon HIL is a hardware in the loop system which produces real hardware results. The model made in MatLab Simulink is an idealized case. Whereas Typhoon uses actual hardware to produce the same curves, and combined with dSPACE give the data in real time.

### 5.2 Solar Panels in Hardware

A disadvantage to using Typhoon is in simulating photovoltaics. There are a limited number of solar panels from which to choose that can be used in the hardware loop. Therefore, the Grape Solar panels from the Simulink mode could not be used. However, two 200 Watt panels were chosen to match as close as possible the behavior of the panels modeled in Simulink. The panels are from Jinko Solar and the model number of the hardware panels is JKM200M. The panel characteristics are summarized in *table 4* and the specification sheet for the solar panel is given in *Appendix 3*.

Maximum Power Pmax	200 W
Voltage at Maximum Power Point Vmpp	36.9 V
Current at Maximum Power Point Impp	5.42 A
Open Circuit Voltage Voc	45.6 V
Short Circuit Current Isc	5.80 A
Temperature Coefficient of Voc	-0.29 %/°C
Temperature Coefficient of Isc	0.05 %/°C

*Table 4 Jinko Solar JKM200M 200 Watt Solar Panel*

Figure 31 is the change in the power max when the temperature of the solar panel changes. Table 5 summarized the value for Temperature and corresponding percent change in power and the predicted power.

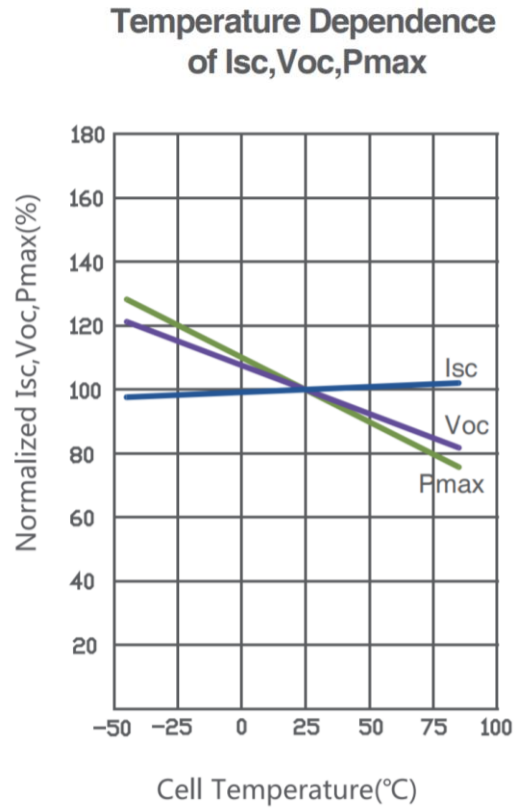


Figure 31 Percent Change in Pmax versus the Cell Temperature

Temperaure (°C)	Change in Pmax (%)	Power (W)
25	100	400
35	96	384
45	92	368
55	88	352

Table 5 Temperature of Solar Panel Corresponding to the relative Change in Power and Value  
for Power

Figure 32 is the IV and PV curve for the Jinko Solar panel at varying irradiances that is provided in the data sheet attached in Appendix 3. Therefore, the estimated values for power can be determined by this graph. Since there are two panels the value for power will be doubled. Table 6 summarizes the expected power of two of the Jinko Solar JKM200M 200 Watt solar panels corresponding to the value of irradiance predicted from figure 33.

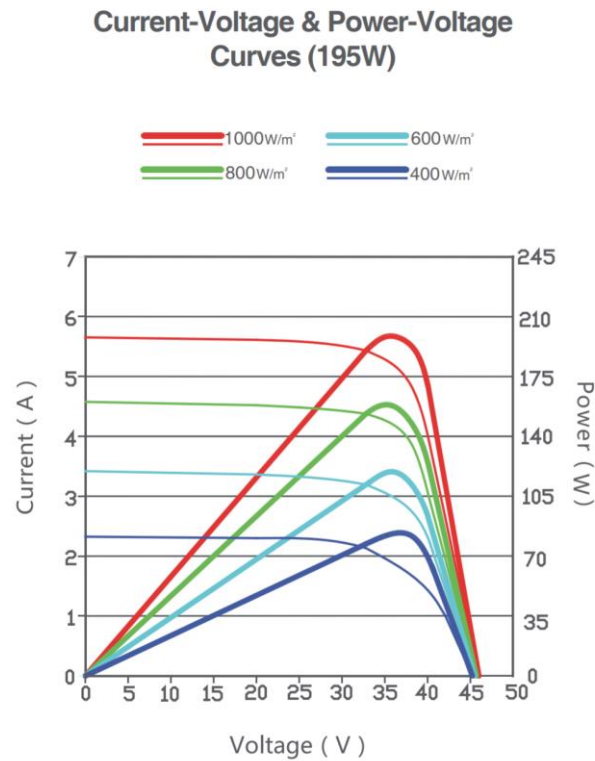


Figure 32 IV and PV Curves at Different Values of Irradiance

Irradiance Value (W/m <sup>2</sup> )	Power (Watts)
1000	400
800	315
600	245
400	175

Table 6 Power Produced by Irradiance for two Jinko Solar JKM200M 200 Watt Solar Panels

## 6 Hardware Results

Although the hardware data is not directly comparable to the data produced by the simulation model there are many behaviors that can be observed that speak to the consistent function of the MPPT. All hardware results are shown through an oscilloscope, measured values relative to time.

Figure 33 shows the hardware adjusting from zero input to conditions of  $1000 \text{ W/m}^2$  at  $25^\circ\text{C}$ . As the value for power increases steps are formed. This behavior within the figure is located within the red brackets. This is the MPPT completing the perturb and observe process in real time, starting at approximately 0 Watts and stepping up and oscillating around 400 Watts. When the system reaches steady state, the oscillation is larger than the oscillation from the Simulink model in figure 16.

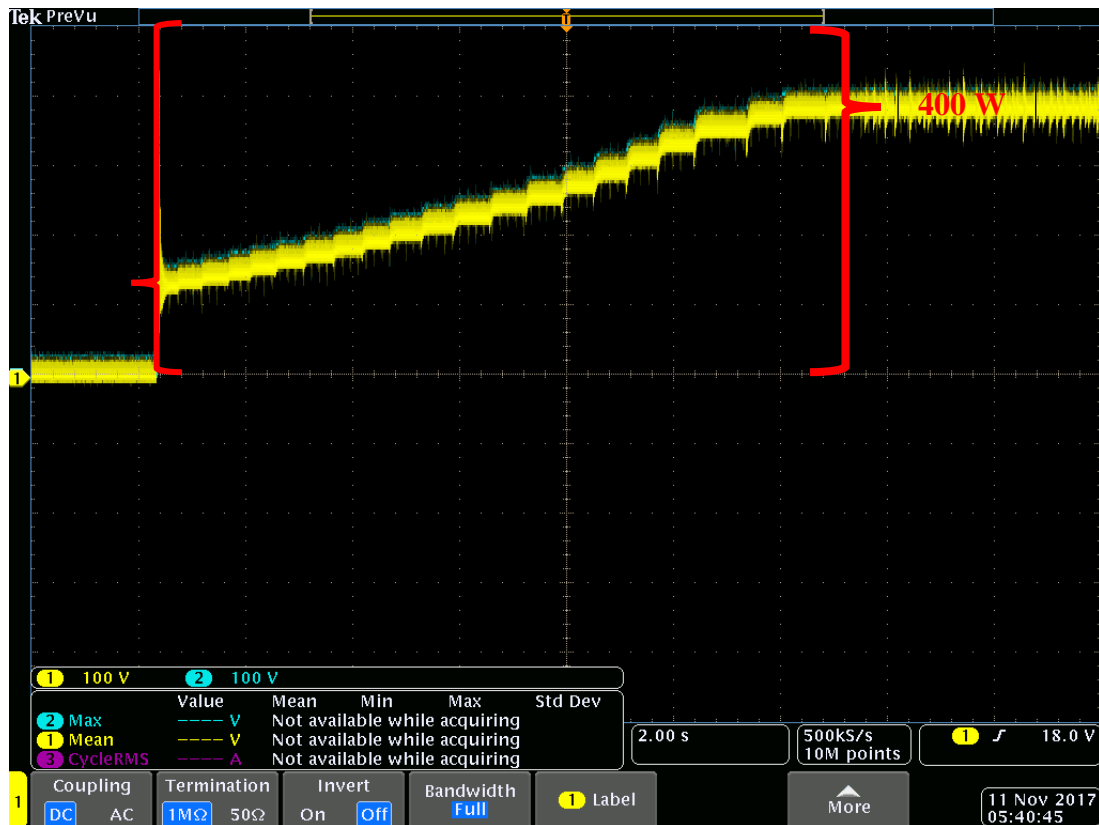


Figure 33 Power versus Time: Simulation Reaching Steady State at  $25^\circ\text{C}$  and  $1000 \text{ W/m}^2$

### 6.1.1 Power: Changing Temperature

Figures 34, 35 and 36 are a 2 second period with a yellow line indicating input power from the solar panels and a blue line indicating the output power after MPPT. The blue output power line is difficult to observe because the input yellow line covers it. This is a result of the MPPT controlling to MPP such that the input and output are balanced. The red arrow indicates the location the values for power change when the temperature is increased.

Figure 34 is the result of increasing the temperature from 25°C to 35°C and displayed on an oscilloscope. The power is in steady state at 25°C, oscillating at approximately 400 Watts. At the red arrow the temperature is increased to 35°C. The power reduces slightly and returns to steady state, but now oscillating around approximately the predicted value of 384 Watts from table 5.



Figure 34 Power versus Time: Increasing Temperature from 25°C to 35°C at 1000 W/m<sup>2</sup>

Figure 35 is the result of increasing the temperature from 35°C to 45°C and displayed on an oscilloscope. The power is in steady state at 35°C, oscillating at approximately 384 Watts. At the red arrow the temperature is increased to 45°C. The power reduces slightly and returns to steady state, but now oscillating around approximately the predicted value of 368 Watts from table 5.

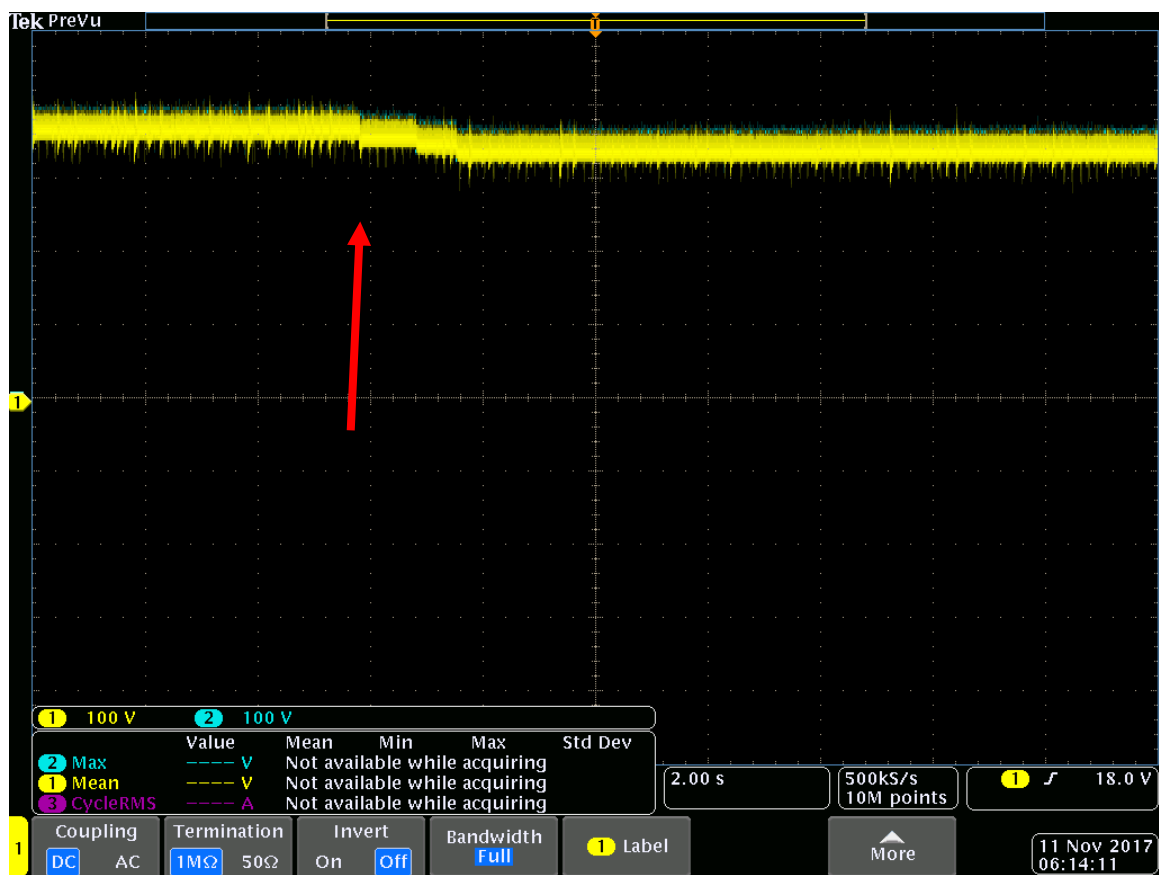


Figure 35 Power versus Time: Increasing Temperature from 35°C to 45°C at 1000 W/m<sup>2</sup>

Figure 36 is the result of increasing the temperature from 45°C to 55°C and displayed on an oscilloscope. The power is in steady state at 45°C, oscillating at approximately 368 Watts. At the red arrow the temperature is increased to 55°C. The power reduces slightly and returns to steady state, but now oscillating around approximately the predicted value of 352 Watts from table 5.

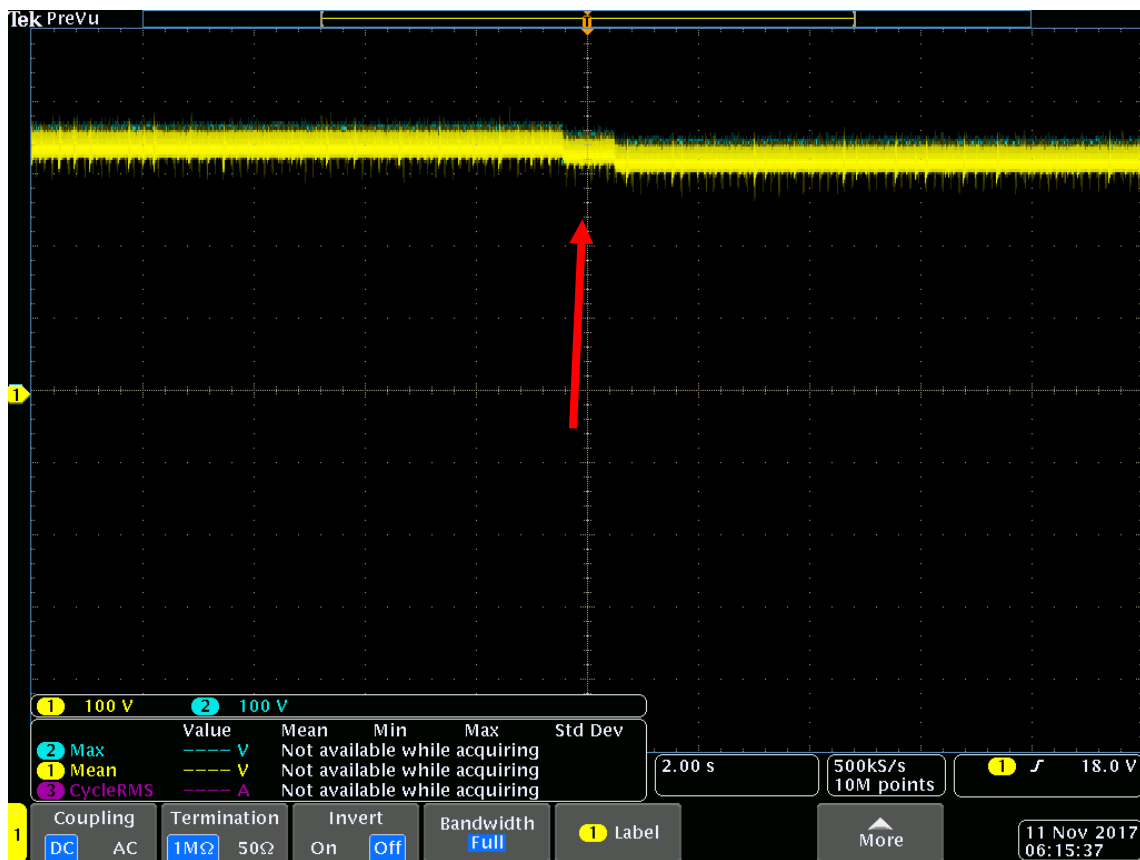


Figure 36 Power versus Time: Increasing Temperature from 45°C to 55°C at 1000 W/m<sup>2</sup>

### 6.1.2 Power: Changing Irradiance

Figures 37, 38, and 39 are a 2 second period with a yellow line indicating input power from the solar panels and a blue line indicating the output power after MPPT. The blue output power line is difficult to observe because the input yellow line covers it. This is a result of the MPPT controlling to MPP such that the input and output are balanced. The red arrow indicates the location the values for power change when the temperature is increased.

Figure 37 is the result of decreasing the irradiance from  $1000\text{W/m}^2$  to  $800\text{W/m}^2$  and displayed on an oscilloscope. The power is in steady state at  $1000\text{W/m}^2$ , oscillating at approximately 400 Watts. At the red arrow the irradiance is decreased to  $800\text{W/m}^2$ . The power reduces and returns to steady state, but now oscillating around approximately the predicted value of 315 Watts from table 6.



Figure 37 Power versus Time: Decreasing Irradiance from 1000 to  $800\text{W/m}^2$  at  $25^\circ\text{C}$



Figure 38 is the result of decreasing the irradiance from  $800\text{W/m}^2$  to  $600\text{ W/m}^2$  and displayed on an oscilloscope. The power is in steady state at  $800\text{W/m}^2$ , oscillating at approximately 315 Watts. At the red arrow the irradiance is decreased to  $600\text{ W/m}^2$ . The power reduces and returns to steady state, but now oscillating slightly lower than the predicted value of 245 Watts from *table 6*.

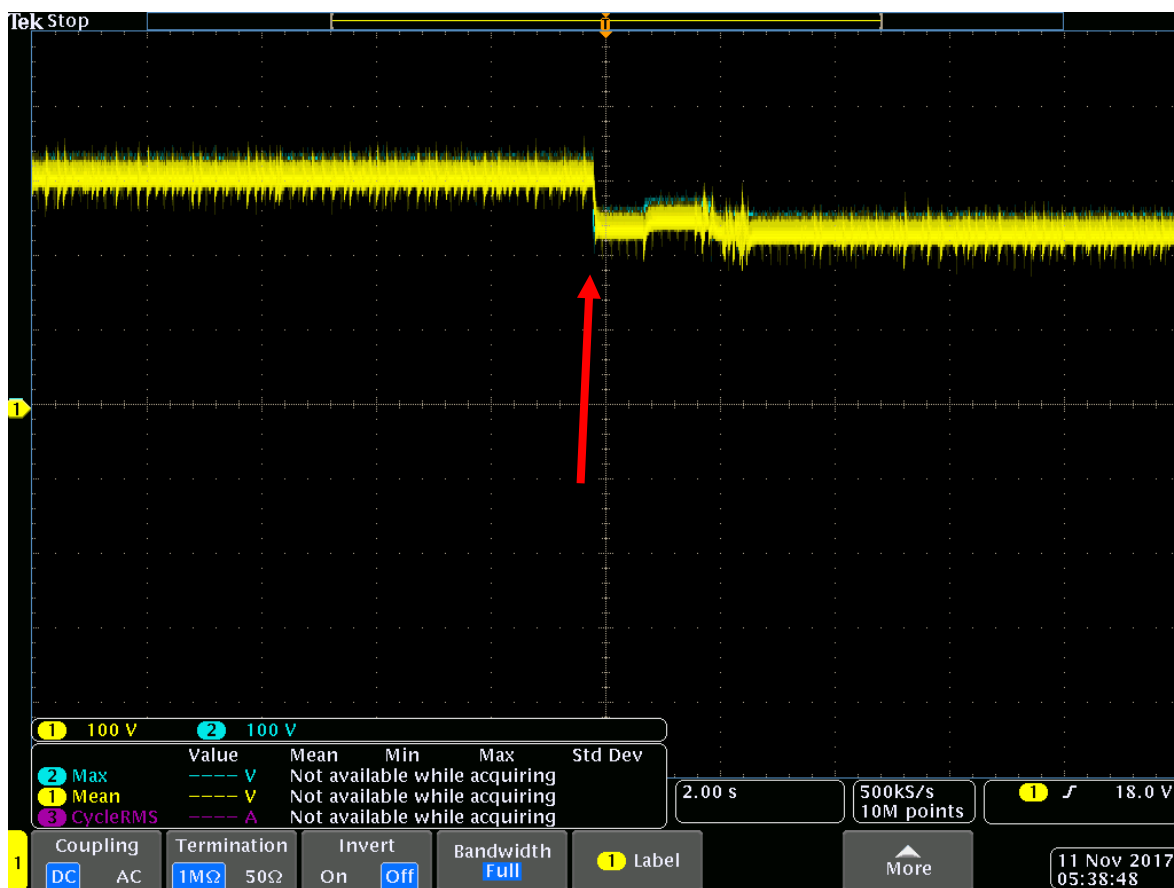


Figure 38 Power versus Time: Decreasing Irradiance from 800 to  $600\text{ W/m}^2$  at  $25^\circ\text{C}$

Figure 39 is the result of decreasing the irradiance from  $600\text{W/m}^2$  to  $400\text{W/m}^2$  displayed on an oscilloscope. The power is in steady state at  $600\text{W/m}^2$ , oscillating slightly lower than 245 Watts. At the red arrow the irradiance is decreased to  $400\text{W/m}^2$ . The power reduces and returns to steady state, but now oscillating much lower than the predicted value of 175 Watts from table 6. At this lowest irradiance value tested the power output is approximately 50 Watts lower than the predicted value.

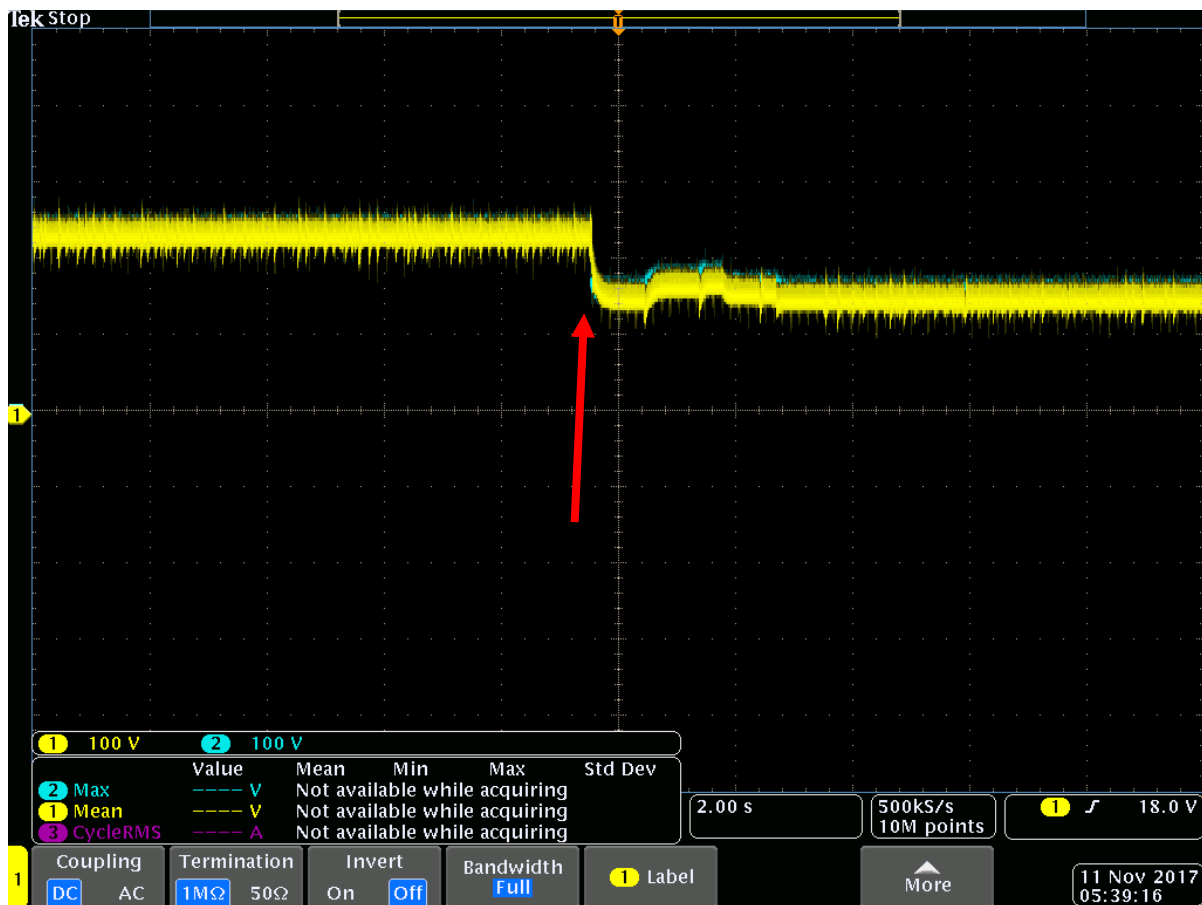


Figure 39 Power versus Time: Decreasing Irradiance from 600 to  $400\text{W/m}^2$  at  $25^\circ\text{C}$

### 6.1.3 Voltage and Current: Changing Temperature

Figure 40 is comprised of two graphs. The bottom graph is a zoomed in, 0.4 second, segment of the upper graph of 2 seconds. The top two lines in each graph are the input current, yellow, and voltage, blue. The bottom two lines are the output current, pink, and voltage green after it has been controlled by the MPPT. The red arrow indicates the location of the values for current and voltage change when the temperature is increase from 25°C to 55°C.

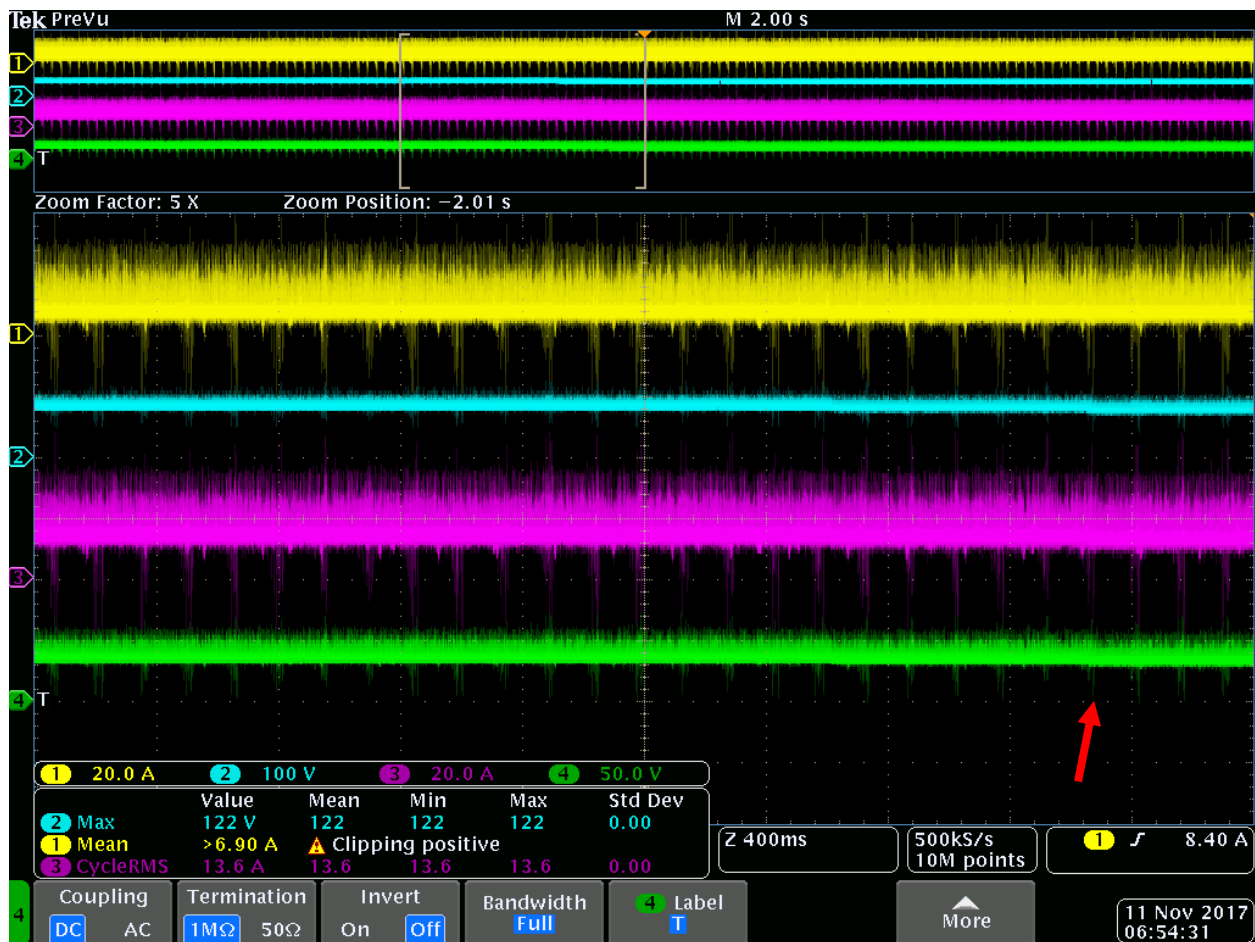


Figure 40 Voltage and Current Input and Output versus Time of Increasing Temperature from 25 to 55°C 1000 W/m<sup>2</sup>

### 6.1.4 Voltage and Current: Changing Irradiance

Figure 41 is comprised of two graphs. The bottom graph is a zoomed in, 0.2 second, segment of the upper graph of 2 seconds. The top two lines in each graph are the input current, yellow, and voltage, blue. The bottom two lines are the output current, pink, and voltage green after it has been controlled by the MPPT. The red arrow indicates the location the values for current and voltage change when the irradiance is decreased from 1000 W/m<sup>2</sup> to 500 W/m<sup>2</sup>.



Figure 41 Voltage and Current Input and Output versus Time of Decreasing Irradiance from 1000 to 500 W/m<sup>2</sup> at 25°C

## 7 Conclusion

The model from MatLab Simulink is useful to optimize the electrical system. The clear results that can be reported and plotted allow for many configurations to be applied and analyzed. However, when compared to the hardware results, the output of the simulation are idealized. The demonstration of the simulation in real time reveals more oscillation within the circuit. Relative to the simulation within MatLab Simulink which shows a much smaller oscillation on the MPPT in steady state.

The results from Typhoon and dSPACE do confirm the operation of the MPPT designed in MatLab Simulink in hardware. The results of the simulation model and the experimental hardware readings are comparable in the performance of the MPPT PO algorithm.

Both simulation and experimentation confirm that the temperature does not cause as much fluctuation in the power output of panels as the irradiance values. However, when in competition this seemingly small amount of power loss due to temperature would result in a lower performance. Therefore, it is important to keep the panels as close to the MPP operating temperature as possible.


The hardware simulation displayed a loss in power at lower irradiances. This makes sense because the system was designed to operate at the maximum output of 400 W. Moreover, the L and C values within the DC to DC converter were found when the panels were operating in ideal conditions. Therefore, when the conditions changed the accuracy of the MPPT was affected.

## References


- [1] Rules of Solar Splash 2018. Lexington, SC: Solar Splash, 2017.
- [2] M. Schmela, "Global Market Outlook for Solar Power 2016-2020," SolarPowerEurope, 2016. [Online]. Available: [http://www.solareb2b.it/wp-content/uploads/2016/06/SPE\\_GMO2016\\_full\\_version.pdf](http://www.solareb2b.it/wp-content/uploads/2016/06/SPE_GMO2016_full_version.pdf). [Accessed: Nov-2017].
- [3] "Solar Cells," Chemistry Explained. [Online]. Available: <http://www.chemistryexplained.com/Ru-Sp/Solar-Cells.html>. [Accessed: 20-Nov-2017].
- [4] K. Zipp and R. M. says, "What are solar panels made of?," Solar Power World, 04-Mar-2016. [Online]. Available: <https://www.solarpowerworldonline.com/2013/05/what-are-solar-panels-made-of/>. [Accessed: 20-Nov-2017].
- [5] V. Salas, E. Olías, A. Barrado, A. Lázaro, "Review of the maximum power point tracking algorithms for stand-alone photovoltaic systems," Solar Energy Materials and Solar Cells, Volume 90, Issue 11, 2006, Pages 1555-1578, ISSN 0927-0248, <http://dx.doi.org/10.1016/j.solmat.2005.10.023>.
- [6] M. G. Villalva, J. R. Gazoli and E. R. Filho, "Modeling and circuit-based simulation of photovoltaic arrays," *2009 Brazilian Power Electronics Conference*, Bonito-Mato Grosso do Sul, 2009, pp. 1244-1254.
- [7] A. Safari and S. Mekhilef, "Simulation and Hardware Implementation of Incremental Conductance MPPT With Direct Control Method Using Cuk Converter," in *IEEE Transactions on Industrial Electronics*, vol. 58, no. 4, pp. 1154-1161, April 2011.
- [8] M. H. Uddin, M. A. Baig and M. Ali, "Comparision of 'perturb & observe' and 'incremental conductance', maximum power point tracking algorithms on real environmental conditions," 2016 International Conference on Computing, Electronic and Electrical Engineering (ICE Cube), Quetta, 2016, pp. 313-317.
- [9] T. Eswam and P. L. Chapman, "Comparison of Photovoltaic Array Maximum Power Point Tracking Techniques," in *IEEE Transactions on Energy Conversion*, vol. 22, no. 2, pp. 439-449, June 2007.
- [10] E. Koutroulis, K. Kalaitzakis and N. C. Voulgaris, "Development of a microcontroller-based, photovoltaic maximum power point tracking control system," in *IEEE Transactions on Power Electronics*, vol. 16, no. 1, pp. 46-54, Jan 2001.
- [11] M. Farahat, H. Metwally, and A. A.-E. Mohamed, "Optimal choice and design of different topologies of DC-DC converter used in PV systems, at different climatic conditions in Egypt," *Renewable Energy*, vol. 43, pp. 393-402, 2012.
- [12] S. S. Ang and A. Oliva, Power-switching converters. Boca Ratón, FL: CRC Press, 2011.

- [13] M. G. Villalva, J. R. Gazoli and E. R. Filho, "Comprehensive Approach to Modeling and Simulation of Photovoltaic Arrays," in *IEEE Transactions on Power Electronics*, vol. 24, no. 5, pp. 1198-1208, May 2009.
- [14] N. Femia, G. Petrone, G. Spagnuolo and M. Vitelli, "Optimization of perturb and observe maximum power point tracking method," in *IEEE Transactions on Power Electronics*, vol. 20, no. 4, pp. 963-973, July 2005.

## Appendix 1: Grape Solar 100 W Specifications



**MODEL: GS-Photoflex-100W**




**Grape Solar®**  
Clean Power. Today.

**High Efficiency Mono-crystalline Flexible Photovoltaic Module**

**Overview**

- High efficiency solar cells with quality silicon material for high module conversion efficiency and long term output stability and reliability.
- Rigorous quality control to meet the highest international standards.
- Outstanding electrical performance under high temperature and weak light environments.



**Applications**


- Any off-grid solar power stations.

**Warranty**

- 1 year limited product warranty on materials and workmanship.
- Refer to warranty document for detailed warranty information.

**Certifications**

- CE



**Mechanical Specifications**

Characteristic	Details
Cell Size	125mm x 125mm (4.92" x 4.92")
Module Dimension (L x W x T)	1050mm x 540mm x 4mm (41.34" x 21.26" x 0.16")
No. of Cells	36
Weight	1.35 kg (3.0 lbs)
Cable Length	900mm (35.4") for positive (+) and negative (-)
Type of Connector	MC-IV comparable
Junction Box	IP65 Rated
No. of Holes in Frame	4 installation holes

Rev.02• 1702



## MODEL: GS-Photoflex-100W

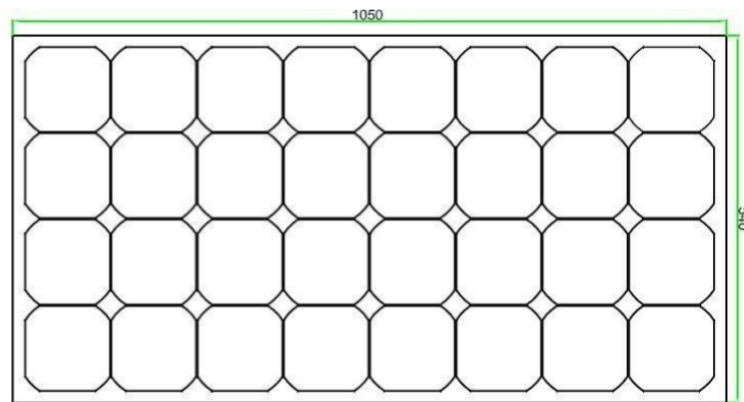
### Electrical Specifications

(STC\* = 25 °C, 1000W/m<sup>2</sup> Irradiance and AM=1.5)

Model	GS-Photoflex-100W
Max Recommended System Voltage	150V
Maximum Power P <sub>max</sub>	100 W* (-10%, +10%)
Cell type	Mono silicon
Voltage at Maximum Power Point V <sub>mpp</sub>	17.8 V
Current at Maximum Power Point I <sub>mpp</sub>	5.62A
Open Circuit Voltage V <sub>oc</sub>	21.6 V
Short Circuit Current I <sub>sc</sub>	5.97 A
Module Efficiency (%)	17.6%
Temperature Coefficient of V <sub>oc</sub>	-0.28% /°C
Temperature Coefficient of I <sub>sc</sub>	+0.04% /°C
Temperature Coefficient of P <sub>max</sub>	-0.38% /°C

\*Standard Test Conditions

### Physical Specifications mm



### Other Performance Data

Power Tolerance	Operating Temperature	Max Series Fuse Rating	NOCT*
-10%, +10%	-40 °C to +85 °C	10A	45 °C +/- 2 °C

\*Normal Operating Cell Temperature

**www.GrapeSolar.com**

For service or support call

**1-541-349-9000**

2635 W. 7th Place

Eugene, Oregon 97402, USA

Tel: 541.349.9000 Fax: 541.343.9000

Grape Solar reserves the rights to modify these specifications without notice.

Rev.02• 1702

## Appendix 2: MatLab Code for PO Method

```
function D = PandO(Param, Va, Ia)
% MPPT controller based on the Perturb & Observe algorithm.
% D output = Duty cycle of the boost converter (value between 0 and 1)
% Enabled input = 1 to enable the MPPT controller
% Va input = PV array terminal voltage (V)
% Ia input = PV array current (A)
% Param input:
Dinit = Param(1); %Initial value for D output
Dmax = Param(2); %Maximum value for D
Dmin = Param(3); %Minimum value for D
deltaD = Param(4); %Increment value used to increase/decrease the duty cycle D
% ( increasing D = decreasing Vref )
persistent Vold Pold Dold;
if isempty(Vold)
Vold=0;
Pold=0;
Dold=Dinit;
end
P= Va*Ia;
dV= Va - Vold;
dP= P - Pold;
if dP > 0
    if dV > 0
        D = Dold + deltaD;
    else
        D = Dold - deltaD;
    end
else
    if dV > 0
        D = Dold - deltaD;
    else
        D = Dold + deltaD;
    end
end

if D >= Dmax || D<= Dmin
    D=Dold;
end
Dold=D;
Vold=Va;
Pold=P;
```

## Appendix 3: Jinko Solar 200 W Specifications

[www.jinkosolar.com](http://www.jinkosolar.com)

**JinKO Solar**  
Building Your Trust in Solar

# JKM215M-72

## 195-215 Watt

MONO CRYSTALLINE MODULE

Positive power tolerance of 0/+3%

ISO9001:2008, ISO14001:2004, OHSAS18001 certified factory.  
IEC61215, IEC61730 certified products.



### KEY FEATURES

**High Efficiency:**  
High module conversion efficiency (up to 16.84%), through innovative manufacturing technology.

**Low-light Performance:**  
Advanced glass and solar cell surface texturing allow for excellent performance in low-light environments.

**Severe Weather Resilience:**  
Certified to withstand: wind load (2400 Pascal) and snow load (5400 Pascal).

**Durability against extreme environmental conditions:**  
High salt mist and ammonia resistance certified by TUV NORD.



PV CYCLE

UL

CE

MCS

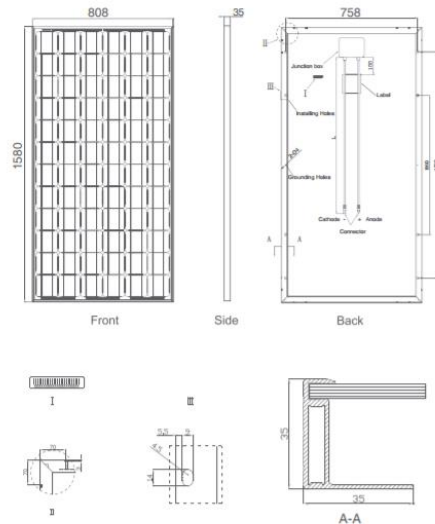
### LINEAR PERFORMANCE WARRANTY

10 Year Product Warranty • 25 Year Linear Power Warranty



Year	Standard performance warranty (%)	Jinko Solar's linear warranty (%)
1	95.0	97.0
5	92.5	94.5
10	90.0	92.0
12	88.5	90.0
25	80.2	80.2

## Engineering Drawings

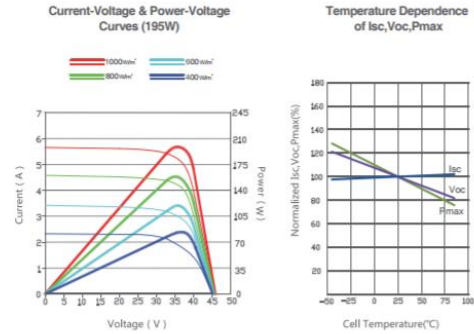


## Packaging Configuration

( Two boxes =One pallet )

28 pcs/box, 56 pcs/pallet, 336 pcs/20'FT Container  
28 pcs/box, 56 pcs/pallet, 784 pcs/40'FT Container

## Electrical Performance & Temperature Dependence



## Mechanical Characteristics

Cell Type	Mono-crystalline 125×125mm (5 inch)
No. of cells	72 (6×12)
Dimensions	1580×808×35mm (62.20×31.81×1.38 inch)
Weight	14.5kg (31.9 lbs.)
Front Glass	3.2mm, High Transmission, Low Iron, Tempered Glass
Frame	Anodized Aluminium Alloy
Junction Box	IP65 Rated
Output Cables	TUV 1×4.0mm <sup>2</sup> , Length:900mm

## SPECIFICATIONS

Module Type	JKM195M		JKM200M		JKM205M		JKM210M		JKM215M	
	STC	NOCT	STC	NOCT	STC	NOCT	STC	NOCT	STC	NOCT
Maximum Power (Pmax)	195Wp	145Wp	200Wp	149Wp	205Wp	153Wp	210Wp	156Wp	215Wp	159Wp
Maximum Power Voltage (Vmp)	36.8V	34.2V	36.9V	34.3V	37.2V	34.6V	37.4V	34.8V	37.7V	35.0V
Maximum Power Current (Imp)	5.30A	4.23A	5.42A	4.33A	5.51A	4.42A	5.61A	4.48A	5.70A	4.54A
Open-circuit Voltage (Voc)	45.4V	42.2V	45.6V	42.4V	45.9V	42.7V	46.1V	42.9V	46.4V	43.2V
Short-circuit Current (Isc)	5.67A	4.56A	5.80A	4.67A	5.90A	4.75A	5.99A	4.82A	6.09A	4.92A
Module Efficiency STC (%)	15.28%		15.67%		16.06%		16.45%		16.84%	
Operating Temperature(°C)	-40°C~+85°C									
Maximum system voltage	1000VDC (IEC)									
Maximum series fuse rating	10A									
Power tolerance	0~+3%									
Temperature coefficients of Pmax	-0.40%/°C									
Temperature coefficients of Voc	-0.29%/°C									
Temperature coefficients of Isc	0.05%/°C									
Nominal operating cell temperature (NOCT)	45±2°C									

STC: Irradiance 1000W/m<sup>2</sup> Cell Temperature 25°C AM=1.5

NOCT: Irradiance 800W/m<sup>2</sup> Ambient Temperature 20°C AM=1.5 Wind Speed 1m/s

\* Power measurement tolerance: ± 3%

The company reserves the final right for explanation on any of the information presented hereby. EN-MKT-215M\_v1.0\_rev2015